Signaling events at TMEM doorways provide potential targets for inhibiting breast cancer dissemination

Chinmay R. Surve[1,5‡], Camille L. Duran[1,2,3,4,‡,*], Xianjun Ye[1,2,3,4,5], Xiaoming Chen[2,3], Yu Lin[2,3], Allison S. Harney[1,5], Yarong Wang[1], Ved P. Sharma[2,5], E. Richard Stanley[6], Dianne Cox[3,4,5,6], John C. McAuliffe[1,2,3,4,7], David Entenberg[1,2,3,4,5], Maja H. Oktay[1,2,3,4,5,7,*] and John S. Condeelis[1,3,4,5,7,8,*]

[1]Integrated Imaging Program for Cancer Research, [2]Department of Pathology, [3]Montefiore Einstein Comprehensive Cancer Center, [4]Cancer Dormancy and Tumor Microenvironment Institute, [5]Gruss-Lipper Biophotonics Center, [6]Department of Developmental and Molecular Biology, [7]Department of Surgery, [8]Department of Cell Biology, Albert Einstein College of Medicine, Bronx, New York. [‡] These authors contributed equally to this work.

***Address for Correspondence:**

Camille L. Duran
Maja H. Oktay
John S. Condeelis
Albert Einstein College of Medicine
Department of Cell Biology
Department of Pathology
1300 Morris Park Ave
Bronx, NY 10461
Email:
camille.duran@einsteinmed.edu
moktay@montiefore.org
john.condeelis@einsteinmed.edu

The authors declare no competing financial interests.

Running Title: TMEM doorway associated targets to inhibit metastasis

Abstract:

Tumor cell intravasation is essential for metastatic dissemination, but its exact mechanism is incompletely understood. We have previously shown that in breast cancer, the direct and stable association of a tumor cell expressing Mena, a Tie2^{hi}/VEGF^{hi} macrophage, and a vascular endothelial cell, creates an intravasation portal, called a "tumor microenvironment of metastasis" (TMEM) doorway, for tumor cell intravasation, leading to dissemination to distant sites. The density of TMEM doorways, also called TMEM doorway score, is a clinically validated prognostic marker of distant metastasis in breast cancer patients. Although we know that tumor cells utilize TMEM doorway-associated transient vascular openings to intravasate, the precise signaling mechanisms involved in TMEM doorway function are only partially understood. Using two mouse models of breast cancer and an *in vitro* assay of intravasation, we report that CSF-1 secreted by the TMEM doorway tumor cell stimulates local secretion of VEGF-A from the Tie2^{hi} TMEM doorway macrophage, leading to the dissociation of endothelial junctions between TMEM doorway associated endothelial cells, supporting tumor cell intravasation. Acute blockade of CSF-1R signaling decreases macrophage VEGF-A secretion as well as TMEM doorway-associated vascular opening, tumor cell trans-endothelial migration, and dissemination. These new insights into signaling events regulating TMEM doorway function should be explored further as treatment strategies for metastatic disease.

49 **Introduction:**

50 Metastasis is a complex, multi-step and multi-directional process that begins with the
51 dissemination of tumor cells from the primary tumor to distant sites and escalates by further re-
52 dissemination of cancer cells from metastatic foci (1-4). The re-dissemination process leads to an
53 exponential increase in tumor burden and, eventually, patient demise. Tumor cell intravasation
54 into the vasculature creates circulating tumor cells (CTCs) and is an essential step in the
55 metastatic cascade, but its exact mechanism is not completely understood. A large body of
56 evidence indicates that tumor cell dissemination, including tumor cell intravasation, is
57 orchestrated by the interaction of tumor cells with the tumor microenvironment (5, 6). In particular,
58 tumor-associated macrophages interact with tumor cells and promote directed cell migration
59 (streaming) towards blood vessels (7-9). In addition, macrophages form a multi-cellular complex
60 with endothelial and tumor cells on the surface of blood vessels to mediate transient vascular
61 opening and tumor cell intravasation. These cell complexes are called TMEM (Tumor
62 MicroEnvironment of Metastasis) doorways (10, 11). Each TMEM doorway is composed of one
63 tumor cell expressing Mena, one Tie2^{hi}/VEGF-A^{hi} macrophage, and a vascular endothelial cell,
64 all in direct and stable physical contact (10, 12, 13).

65 TMEM doorway-associated vascular opening (TAVO) was first discovered using high-
66 resolution intravital imaging as localized and transient bursts of intravascular contrast agents into
67 the extravascular space that could be accompanied by concurrent intravasation of cancer cells
68 (10). Further analyses revealed in mouse models of breast cancer, TAVO, and its associated
69 cancer cell intravasation, occurs exclusively at TMEM doorways (10). Importantly, TMEM
70 doorway score in primary breast tumors has been clinically validated as a prognostic marker of
71 distant metastatic recurrence in breast cancer patients with estrogen receptor positive HER2
72 negative (ER^{+}/HER2^{-}) disease, independent of other clinical prognostics (12-14). Additionally,
73 when comparing residual ER^{+}/HER2^{-} tumors from breast cancer patients after completion of pre-
74 operative chemotherapy, Black patients were found to have a higher TMEM doorway score than

75 white patients (15). These findings potentially provide an explanation for the persistent racial
76 disparities in $ER^+/HER2^-$ breast cancer outcomes that are not fully explained by disparities in
77 social determinants of health, including access to care or treatment (12, 15-17). TMEM doorway
78 score has also been found to increase during neo-adjuvant chemotherapy, suggesting that TMEM
79 doorway score, as measured using TMEM doorway activity MRI (17), may be a useful companion
80 diagnostic for the prediction of benefit from certain types of treatment. Given that Black compared
81 to white patients have a higher TMEM doorway density in their residual disease after
82 chemotherapy, using TMEM doorway activity MRI may potentially help diminish racial disparity in
83 breast cancer outcome (18, 19).

84 In humans and mice, TMEM doorways are found in pre-invasive and invasive ductal breast
85 carcinoma, as well as in metastatic foci in lymph nodes and lungs (18-24). This suggests that the
86 TMEM doorway-mediated mechanism of cancer cell dissemination occurs not only at the primary
87 tumor site, but also at metastatic sites, and may contribute to the multi-directional cancer spread
88 that perpetuates metastatic dissemination even after removal of the primary tumor (1-4, 18). Thus,
89 understanding the molecular mechanisms of TMEM doorway function may help develop
90 therapeutic targets to slow distant metastases and improve patient survival.

91 Inhibiting TAVO prevents the formation of CTCs and metastases (10). Although we know that
92 TMEM doorways induce localized vascular opening through the secretion of vascular endothelial
93 growth factor-A (VEGF-A) from the TMEM doorway macrophage (10), the precise signaling
94 mechanisms involved in TMEM doorway function during intravasation have not been elucidated.
95 The work described here provides a greater understanding of the signaling events that regulate
96 these dynamic, multi-cellular interactions. In particular, we report the identification of the signaling
97 events involved in TAVO and TMEM doorway-mediated intravasation, which can serve as
98 potential new prognostic markers and therapeutic targets for suppressing CTC dissemination and
99 breast cancer metastasis.

100

101 **Materials and Methods:**

102 ***Cell culture.*** MDA-MB-231 cells were cultured in Dulbecco's Modified Eagle Medium (DMEM)
103 (cat# SH30243, Hyclone, GE Healthcare Life Sciences, Logan, UT, USA) supplemented with 10%
104 fetal bovine serum (FBS) (cat# S11550, Atlanta Biologicals, Flowery Branch, GA, USA).
105 BAC1.2F5 macrophages (67) and bone marrow derived macrophages (BMMs) were cultured in
106 Minimum Essential Medium, Alpha (α-MEM) (cat# 15-012-CV, Corning, Tewksbury, MA, USA)
107 supplemented with 10% FBS (cat# 100-106, Gemini Bio-Products, Sacramento, CA, USA) and
108 36 µg/mL CSF-1 (3000 units/mL, a gift from Dr. E. Richard Stanley). Immortalized BMMs derived
109 from *Csf1r*$^{+/+}$ and *Csf1r*$^{-/-}$ mice have been previously described (33), and were cultured in α-MEM
110 supplemented with 10% FBS and GM-CSF. Human Umbilical Vein Endothelial Cells (HUVECs)
111 were cultured in complete EGM-2 (cat# CC-3162, Lonza, Allendale, NJ, USA) and were not used
112 beyond passage five for any experiments.

113

114 ***Mice.*** All studies involving mice were conducted in accordance with the National Institutes of
115 Health regulations concerning the care and use of experimental animals. The procedures were
116 approved by the Albert Einstein College of Medicine Institute for Animal Care and Use Committee.
117 Transgenic mice expressing the Polyoma Middle T (PyMT) antigen under the control of the
118 mammary tumor virus long terminal repeat (MMTV-LTR) (68) were bred in house.

119 ***Inhibitors.*** Inhibitors were administered based on established doses of efficacy found in previous
120 studies. Animals were treated with 2.5 µg of anti-CSF-1R neutralizing antibody (cat# NBP1-
121 43363, clone AFS98, Novus Biologicals, Centennial, CO, USA), or antibody isotype control (cat#
122 554682, IgG K isotype control, BD Pharmingen, Franklin Lakes, NJ, USA) was administered by
123 tail vein *i.v.* four hours before termination of the experiment as previously described (27). For *in*
124 *vitro* studies, GW2580 a small molecule inhibitor of CSF-1R (cat# G-5903, LC Laboratories,
125 Woburn, MA, USA) was dissolved in DMSO was used at a concentration of 100 nM, and anti-

126 CSF-1R neutralizing antibody or isotype control (clone AFS98, Novus Biologicals) was used at a
127 concentration of 50 ng/mL

128 ***Immunofluorescence labeling of tumor vasculature and extravasation with 155 kDa***
129 ***dextran-TMR.*** Labeling flowing vasculature and sites of permeability was performed as previously
130 described (10). Briefly, to quantify extravasation, high molecular weight 155 kDa TMR-dextran
131 (cat# T1287, Sigma-Aldrich, Burlington, MA, USA) diluted in PBS was administered by tail vein
132 *i.v.* one hour before the termination of the experiments. Anti-mouse CD31-biotin (cat# 13-0311-
133 82, Thermo Fisher, Waltham, MA, USA) was administered by tail vein *i.v.* ten minutes before the
134 end of the experiment to label flowing blood vessels. At time of sacrifice tumors were removed
135 and fixed for 48 hours in 10% formalin in a volume ratio of tumor to formalin of 1:7 and made into
136 paraffin blocks. Paraffin blocks of tumors were cut into 5 μm sections and immunofluorescence
137 staining was performed. TMR-Dextran is visualized using rabbit anti-TMR (A-6397; Life
138 Technologies, Carlsbad, CA, USA).

139 ***Immunofluorescence staining of tissue.*** Tumor sections were dewaxed in acetone and
140 rehydrated in alcohol followed by water. Antigen retrieval was performed with a citrate solution at
141 pH 5.5 in a humidified chamber. The slides were washed with PBS-T (0.1% Tween-20) and
142 blocked with a blocking solution (2% BSA, 10% FBS in PBS). One 5 μm section from each tumor
143 was stained for hematoxylin and eosin (H&E) and one for TMEM doorway. TMEM doorway stain
144 is a triple immuno-stain for predicting metastatic risk, in which three antibodies are applied
145 sequentially and developed separately with different chromogens on a Dako Autostainer (13, 14,
146 32). The following primary antibodies were used for immunostaining of TMEM doorways: anti-
147 Mena (cat# NBP1-87914, Novus Biologicals), anti-endomucin (cat# sc-65495, Santa Cruz
148 Biotechnology, Dallas, TX, USA), and anti-CD68 (cat# MCA1957, clone FA-11, Serotec,
149 Kidlington, UK), or anti-Iba1 (anti-Iba1 (cat# 019-19741, FUJIFILM Wako Chemicals, Richmond,

150 VA). The sequential tissue sections were stained with different combinations of: anti-endomucin
151 (cat# sc-65495, Santa Cruz Biotechnology), anti-TMR (to visualize TMR-dextran, cat# A-6397,
152 Thermo Fisher Scientific), anti-ZO-1 (cat# MABT11, clone R40.76, Millipore Sigma), anti-CD31
153 (cat# 77699; Cell Signaling Technology, Danvers, MA, USA), Red fluorochrome(635)-conjugated
154 anti-Iba1 (cat# 013-26471, FUJIFILM Wako Chemicals), or anti-Iba1 (cat# 019-19741, FUJIFILM
155 Wako Chemicals), anti-VEGF-A (cat# sc-152, clone A-20, Santa Cruz Biotechnology) or anti-
156 VEGF-A (cat#512809, clone 2G11-2A05, Biolegend, San Diego, CA, USA), anti-CSF-1R (cat#
157 sc-692, clone C-20, Santa Cruz Biotechnology), AlexaFluor555-conjugated anti-CSF-1 (cat# bs-
158 4910R-A555, Bioss Inc, Woburn, MA, USA), anti-CD68 (cat# MCA1957, clone FA-11, Serotec),
159 or AlexaFluor647-conjugated CD68 (cat#51-0689-42, eBioscience, San Diego, CA, USA), and
160 anti-MRC1/CD206 (cat# AF2535, R&D Systems, Minneapolis, MN, USA). Sections were washed
161 with PBS-T and the primary antibodies were detected with AlexaFluor 488, 555 or 647 conjugated
162 secondary antibodies targeting the primary antibody species (Invitrogen, Eugene, OR, USA), and
163 nuclei were stained with 4, 6-diamidino-2-phenylindole (DAPI). All fluorescently labeled samples
164 were mounted with Prolong Diamond antifade reagent (cat# P36961, Invitrogen) and imaged with
165 a PerkinElmer Pannoramic 250 Flash II digital whole-slide scanner using a 20x 0.8NA Plan-
166 Apochromat objective (PerkinElmer, Hopkinton, MA, USA). Images of individual fields of view
167 were imported into ImageJ or VisioPharm for analysis. TMEM doorways were identified as
168 previously described (10, 13, 14). Vascular junctions and extravascular dextran were quantified
169 as previously described (10, 30). Briefly, the CD31 channel (blood vessel), dextran and vascular
170 junction (ZO-1) were each thresholded to just above background based upon intensity and by
171 comparison to a slide stained only with secondary antibodies. A binary mask was created for the
172 CD31 positive staining (blood vessel mask) and for the dextran positive staining (dextran mask).
173 The extravascular dextran area was isolated by subtracting the blood vessel mask from the
174 dextran mask. The remaining extravascular dextran area and blood vessel area were then
175 measured.

176 ***Extravascular dextran, VEGF-A, and intracellular CSF-1 quantification in TMEM doorways.***
177 To identify active TMEM doorways, we utilized an improved and automated method of a prior
178 TMEM activity assay that takes into account the presence of high-molecular weight dextran that
179 leaks into the tissue, as a result of TMEM doorway associated vascular opening (TAVO) (10, 30,
180 31). The algorithmic improvement of this assay involves the automated measurement of the entire
181 tissue section of the tumor as a single region of interest (ROI), instead of selecting a definite
182 number of high power fields as ROIs, thus providing a more accurate representation of the entire
183 tumor, minimizing operator-dependent biases, and significantly increasing the logistic capacity of
184 the analysis.

185 In short, serial tissue sections were cut and stained for TMR-Dextran, CSF-1, and Endomucin by
186 IF (tissue section 1) and for TMEM doorways by staining for Iba1, Endomucin, and panMena by
187 IHC (tissue section 2). The sections were then imaged with a digital whole slide scanner and
188 aligned to the single cell level using the TissueAlign module in Vis (Visiopharm, Hoersholm,
189 Denmark). IF images were thresholded above background, creating binary masks for endomucin
190 (blood vessel) and dextran signals. These masks were then superimposed so as to be able to
191 differentiate between intravascular and extravascular dextran signal. In the IHC section, TMEM
192 doorways were identified using previously published criteria (13, 14). In this manner, the amount
193 of extravascular dextran around TMEM doorways could be quantified. For quantification of
194 intracellular CSF-1, the TMEM doorway associated tumor cell was identified using the Mena stain
195 in IHC section, within the TMEM doorway circle, and a mask was created. This mask was then
196 overlaid onto the aligned IF section and the CSF-1 was then quantified within this mask.

197 ***siRNA knockdown.*** MDA-MB-231 cells were transfected with Stealth RNAi siRNAs (siRNA IDs:
198 HSS102355, HSS102356, HSS175321, Thermo Fisher Scientific) directed against CSF-1 or

199 negative control (cat#12935300, Thermo Fisher Scientific) at a concentration of 200 pmols using
200 Lipofectamine 2000 reagent (cat# 11668027, Invitrogen).

201 ***Immunofluorescence staining of co-cultured cells***. Prior to the start of the experiment,
202 macrophages were labeled with CellTracker Green™ dye and tumor cells were labelled with
203 CellTracker™ Red dye, according to manufacturer's instructions (cat# C7025, C34552,
204 Invitrogen). $1x10^5$ macrophages were cultured with or without $1x10^5$ tumor cells in α-MEM media
205 (supplemented with 0.5% FBS and 300 units/mL of CSF-1) and with either CSF-1R blocking
206 antibody or isotype control antibody at 50 ng/mL (cat# NBP1-43363, clone AFS98, Novus
207 Biologicals; IgG K isotype control cat# 554682, BD Pharmingen). After 24 hours incubation, the
208 experiments were stopped by washing the cells with ice-cold PBS followed by fixing them for
209 twenty minutes in 4% PFA, and permeablizing in 0.1% Triton X-100 in PBS. The cells were stained
210 for VEGF-A using antibodies against mouse VEGF-A (cat# 512809, clone 2G11-2A05, Biolegend)
211 and AlexaFluor647-conjugated secondary antibodies. The intensity of VEGF-A staining in the
212 macrophages was measured by first outlining the macrophages in the green (488 nm) channel in
213 ImageJ/Fiji (69) and applying that outline to the far-red (647 nm) channel to measure the VEGF-
214 A signal within the macrophage, excluding any VEGF-A signal from the tumor cells.

215 ***Quantitative real-time polymerase chain reaction (qPCR).*** To quantify gene expression in
216 MDA-MB-231 tumor cells transfected with CSF-1 siRNA or control siRNA, tumor cells were grown
217 under normal culture conditions. In co-culture experiments between tumor cells and
218 macrophages, $1x10^6$ macrophages were cultured alone or co-cultured with $1x10^6$ MDA-MB-231
219 tumor cells for 24 hours in α-MEM media with 0.5% FBS and 300 units/mL of CSF-1 (one-tenth
220 of CSF-1 added to complete media). For the co-culture assay, species specific primers were used
221 in the qPCR.

222 Total RNA was isolated from cells by using the RNeasy Plus Mini Kit (cat# 74134, Qiagen,
223 Germantown, MD, USA) and cDNA was synthesized and amplified from 1 µg total RNA using the
224 using SuperScript IV VILO Master Mix with ezDNase Enzyme (cat# 11766050, Thermo Fisher
225 Scientific) per manufacturer's protocol. The qPCR was performed with SYBR Green PCR Master
226 Mix (cat# 4367659, Thermo Fisher Scientific) using a QuantStudio 3 real-time PCR instrument
227 (applied biosystems, Thermo Fisher Scientific). The following primers were used: mouse GAPDH
228 5'- CTCATGACCACAGTCCATGC -3', 5'- CACATTGGGGGTAGGAACAC -3'; mouse VEGF-A
229 5'- AGCAGAAGTCCCATGAAGTGA -3', 5'- ATGTCCACCAGGGTCTCAAT -3'; human GAPDH
230 5'- CTCCTGTTCGACAGTCAGCC -3', 5'- ACCAAATCCGTTGACTCCGAC -3'; human β-Actin 5'-
231 CTTCGCGGGCGACGATGC -3', 5'- CGTACATGGCTGGGGTGTTG -3'; human CSF-1 5'-
232 CCTCCCACGACATGGCT -3', 5'- GAGACTGCAGGTGTCCACTC -3'. The mean cycle threshold
233 (Ct) values were then used to analyze relative expression. Analysis was performed using
234 comparative-CT method ($2^{-\Delta CT}$ method) and all Ct values were normalized to GAPDH. Each
235 reaction was performed in triplicate.

236 ***ELISA.*** In macrophage-tumor cell co-culture experiments, $1x10^6$ macrophages were cultured
237 alone or co-cultured with $1x10^6$ MDA-MB-231 tumor cells for up to 48 hours in α-MEM media with
238 0.5% FBS and 300 units/mL of CSF-1 (one-tenth of CSF-1 added to complete media).
239 Experiments using immortalized *Csf1r*$^{+/+}$ or *Csf1r*$^{-/-}$ BMMs used α-MEM media with 0.5% FBS and
240 2 ng/mL GM-CSF. In mono-culture macrophage ELISA experiments where tumor cell conditioned
241 media was added, conditioned media was collected from tumor cells incubated in α-MEM with
242 0.5% FBS and 300 units/mL of CSF-1 for 24 hours. In tumor cell mono-culture ELISA experiments,
243 $1x10^6$ tumor cells were seeded and incubated for 24 hours in serum-free DMEM medium.

244 In all ELISA experiments, blocking antibodies, isotype controls, inhibitors and controls were added
245 at indicated concentrations in "Inhibitors" section, at time zero. Media conditioned by the cultured

246 cells were collected at the indicated time points and stored at -80^{0}C until use. ELISAs were
247 performed per the manufacturer's recommendations using the Mouse VEGF-A DuoSet ELISA kit
248 (cat# DY493, R&D Systems) or the Human M-CSF DuoSet ELISA kit (cat# DY216, R&D
249 Systems). The concentration of protein secreted was interpolated from the standard curve
250 measurements.

251 ***Transendothelial Migration Assay (iTEM assay)***. The iTEM assay was performed as previously
252 described (34, 70, 71) and briefly described here. The transwell (8 µm pore size; cat# 353097,
253 Corning, Corning, NY, USA) was prepared so that tumor cell transendothelial migration was in
254 the intravasation direction found *in vivo* (from subluminal side to luminal side of the endothelium).
255 To prepare the endothelial monolayer, the underside of each transwell was coated with 50 µL of
256 Matrigel (2.5 µg/mL; cat# 354230, Corning). Approximately 1x10^5 HUVECs were plated on the
257 Matrigel coated underside of the transwell. Transwells were then flipped into a 24-well plate
258 containing 200 µL of EGM-2 and monolayers were formed over a 48 hour period. The integrity of
259 the endothelium was measured using low molecular weight dextran as described previously (71).
260 Macrophages and tumor cells were labelled with cell tracker dyes (cat# C7025, C34552,
261 Invitrogen) before the experiment. Then, 1.5x10^4 tumor cells and 6x10^4 macrophages were added
262 to the upper chamber of the transwell in 200 µL of DMEM without serum while the bottom chamber
263 contained EGM-2 supplemented with 36 µg/mL of CSF-1. After 18 hours, the transwells were
264 fixed and stained for ZO-1 (cat# 402200, Invitrogen) as previously described. Transwells were
265 imaged using a Leica SP5 confocal microscope using a 60x 1.4NA objective and processed using
266 ImageJ/Fiji (69). Tumor cell transendothelial migration quantification was performed by counting
267 the number of tumor cells that had crossed the intact endothelium (intact monolayers confirmed
268 by ZO-1 staining for tight junctions) within the same field of view (60x, 10 random fields) and
269 represented as normalized values from at least three independent experiments.
270

271 ***Statistical analysis.*** Individual animals in each cohort are presented as individual points on a dot
272 plot. A horizontal line indicates the mean value and the error bars represent the standard error of
273 the mean. Statistical significance was determined using an unpaired Student's *t*-test, one-way
274 ANOVA, or two-way ANOVA, with Tukey's multiple comparisons test, as indicated, using
275 GraphPad Prism (version 10; Graph Pad Software, La Jolla, CA). Data sets were checked for
276 normality (D'Agostino & Pearson omnibus normality test or Shapiro-Wilk normality test) and
277 unequal variance using GraphPad Prism. Welch's correction was applied to *t*-tests as needed. *P*
278 values less than 0.05 were deemed significant. For *in vitro* experiments, results are representative
279 of at least three independent experiments.

280 **Results:**

281 **CSF-1 levels are elevated in tumor cells at active TMEM doorways**

282 Macrophage-secreted VEGF-A is critical for regulation of TMEM doorway activity (10).
283 VEGF-A secreted by macrophages is regulated by CSF-1, also known as M-CSF (25, 26). Since
284 tumor cells are known to secrete CSF-1 (27-29), we investigated if TMEM doorway tumor cells
285 express CSF-1, and if this expression is associated with TMEM doorway vascular opening (10).
286 We first determined whether CSF-1 levels are increased in TMEM doorway tumor cells at active
287 TMEM doorways by multiplex staining of breast tumor tissue sections obtained from the *polyoma*
288 middle T antigen (PyMT) mice injected *i.v.* with high molecular weight dextran (155 kDa, green)
289 1 hour before sacrifice. In these samples, if there has been a TMEM doorway associated vascular
290 opening (TAVO) (which would indicate an active TMEM doorway), the *i.v.* injected dextran would
291 extravasate into the interstitium and be detectable extravascularly in the tissue near a TMEM
292 doorway **(Figure 1A)**. We used a modified approach of our previously published protocol for
293 detection of active TMEM doorways (30). We stained two sequential tumor sections – one using
294 IHC for TMEM doorways (Iba1, Endomucin, Mena) **(Figure 1B)** and the second using IF for CSF-
295 1, dextran, and endothelial cells (endomucin) **(Figure 1C)** and aligned the images of stained

296 sections to the single cell level. Next, we identified which TMEM doorways were active by
297 examining for the presence of high molecular weight dextran (155 kDa, green) in the extravascular
298 space near the TMEM doorway, as described previously (10, 31). We then visualized and
299 quantified the expression of CSF-1 (red) in TMEM doorway tumor cells of both active and inactive
300 doorways **(Figure 1C)**. We observed that the fluorescence intensity of intracellular CSF-1 in
301 TMEM doorway tumor cells was higher in active TMEM doorways **(Figure 1C, lower panel)**
302 compared to inactive TMEM doorways **(Figure 1C, upper panel)**. This is quantified in **Figure 1D**.
303 These results indicate that TMEM doorway tumor cells may play a significant role in regulating
304 TMEM doorway function and activity by locally producing CSF-1.
305

306 **Tumor cells stimulate macrophage VEGF-A secretion without affecting its expression**

307 Since CSF-1 is upregulated in the tumor cell at active TMEM doorways, and secretion of
308 VEGF-A is known to be regulated by CSF-1 in other cell types (25, 26), we investigated the
309 signaling interplay between the tumor cell and macrophage at the TMEM doorway. Using an
310 ELISA on conditioned media, we confirmed that exogenous recombinant CSF-1 can stimulate
311 macrophages to secrete VEGF-A **(Figure 2A)** and that tumor cells secrete CSF-1 **(Figure 2B)**.
312 To examine the role of tumor cell secreted CSF-1 in regulating macrophage VEGF-A secretion,
313 we first determined if TMEM doorway macrophages express the CSF-1 receptor (CSF-1R). We
314 have previously identified TMEM doorway macrophages by their direct contact with a tumor cell
315 and blood vessel (13), expression of CD68 and VEGF-A, and further characterized them as a
316 $CD206^+/CD11b^+/F4/80^+/CD11c^-$ population (10). Using immunofluorescence staining of PyMT
317 tumors for CSF-1R, macrophages ($CD68^+/CD206^+/CD31^-$), and endothelial cells ($CD31^+$) as
318 described previously (10, 32), we found that greater than 90% of all $CD68^+$ macrophages
319 throughout the tumor tissue co-express CSF-1R and 97% of $CD68^+/CD206^+$ TMEM doorway
320 macrophages (identified by simultaneous contact with tumor cells and endothelial cells and co-
321 expression of CD68 and CD206 without CD31 expression) also express CSF-1R **(Figure 2C, D)**.

322 To determine if tumor cells can stimulate macrophage VEGF-A secretion, we used a
323 human tumor cell - mouse macrophage co-culture system and quantified the amount of secreted
324 VEGF-A by ELISA using an antibody that can only recognize mouse-derived VEGF-A, secreted
325 by the macrophages. Co-culture of human MDA-MB-231 tumor cells with mouse BAC1.2F5
326 macrophages **(Figure 3A)** or culture of BAC1.2F5 macrophages with conditioned media collected
327 from serum starved MDA-MB-231 tumor cells **(Figure 3B)**, resulted in increased secretion of
328 VEGF-A by the mouse-derived macrophages.

329 To ascertain the role of tumor cell secreted CSF-1 in stimulating macrophage VEGF-A
330 secretion, we used the same co-culture system of MDA-MB-231 tumor cells and BAC1.2F5
331 macrophages as above. We inhibited CSF-1R signaling in macrophages with either a CSF-1R
332 neutralizing antibody (CSF-1R Ab), or an inhibitor which prevents downstream signaling of the
333 CSF-1R (CSF-1R inhibitor (GW2580)). We found that either method reduced macrophage VEGF-
334 A secretion **(Figure 3A)**. Likewise, inhibition of CSF-1R in macrophages cultured with medium
335 conditioned by the tumor cells led to a reduction in the amount of secreted VEGF-A **(Figure 3B)**.
336 Similar results were obtained using mouse bone marrow derived primary macrophages (BMMs)
337 **(Supplementary Figure 1A)**. Co-culturing a different breast cancer cell line, 4T1, which also
338 secretes CSF-1 **(Supplementary Figure 1B)**, with BAC1.2F5 macrophages also caused an
339 increase in VEGF-A secretion by macrophages **(Supplementary Figure 1C).** In these additional
340 models, the increase in macrophage secretion of VEGF-A in response to tumor cell CSF-1 was
341 again suppressed through addition of CSF-1R inhibitors or blocking antibodies **(Supplemental**
342 **Figure 1A, 1C)**. Next, we used immortalized bone marrow macrophages (BMMs) isolated from
343 *Csf1r*$^{+/+}$ or *Csf1r*$^{-/-}$ mice which either express (*Csf1r*$^{+/+}$) or lack the expression of CSF-1R (C*sf1r*$^{-/-}$
344 *)* (33) to determine the role of the CSF-1R in regulating VEGF-A secretion by macrophages.
345 Compared to the *Csf1r*$^{+/+}$ BMMs, which secreted VEGF-A in both the co-culture system and when
346 cultured in tumor cell conditioned media **(Figure 3C, D)**, C*sf1r*$^{-/-}$ BMMs did not significantly secrete

347 VEGF-A, in either a co-culture system with MDA-MB-231 tumor cells, or when cultured with
348 medium conditioned by the tumor cells **(Figure 3C, D)**.

349 We next evaluated if co-culture of tumor cells with macrophages leads to increased
350 expression or secretion of VEGF-A from macrophages, or both. We co-cultured MDA-MB-231
351 tumor cells with BAC1.2F5 macrophages labeled with CellTracker™ Green to distinguish them
352 from cancer cells, and then stained the cells for VEGF-A. Macrophages that were co-cultured with
353 tumor cells displayed decreased intracellular VEGF-A staining compared to macrophages
354 cultured alone **(Figure 3E, F)**. This result, combined with the VEGF-A ELISA showing that
355 macrophages and tumor cells cultured in the same method lead to increased VEGF-A in the
356 conditioned media (Figure 3A), suggests that the tumor cells induce macrophages to secrete
357 VEGF-A. In addition, inhibition of CSF-1R signaling (which prevented VEGF-A secretion in Figure
358 3A) increased the intracellular macrophage VEGF-A using the same co-culture system **(Figure
359 3E, F)**, indicating that the CSF-1/CSF-1R signaling between macrophages and tumor cells
360 induces the release of intracellular VEGF-A from macrophages. In our second model using 4T1
361 tumor cells, we again found a decrease in intracellular VEGF-A staining in the macrophages co-
362 cultured with tumor cells compared to macrophages cultured without tumor cells **(Supplementary
363 Figure 1D).** The increase in macrophage VEGF-A secretion and the decrease in the intracellular
364 VEGF-A protein levels in the macrophages were abrogated with CSF-1R neutralizing antibody as
365 well as with the small molecule CSF-1R inhibitor, consistent to what was observed with MDA-MB-
366 231 cells in **Figure 3**.

367 To determine if the enhancement of VEGF-A secreted by the macrophages in response
368 to co-culture with tumor cells could also be due to increased VEGF-A mRNA production, we co-
369 cultured MDA-MB-231 tumor cells with BAC1.2F5 macrophages and determined the relative
370 levels of VEGF-A mRNA by qPCR. We found that co-culture of tumor cells and macrophages did
371 not affect the VEGF-A mRNA levels in macrophages **(Supplementary Figure 2)**, indicating that
372 the increase in VEGF-A protein found in the conditioned medium was due to increased secretion

373 of stored intracellular VEGF-A in the macrophages, not also caused by an increase in VEGF-A
374 mRNA expression.

375 To determine the impact of CSF-1R inhibition on the levels of VEGF-A expression *in vivo*,
376 we treated mice with either a control or a CSF-1R inhibitory antibody and looked at the total level
377 of VEGF-A (both intra- and extracellular) within TMEM doorways. We found that CSF-1R inhibition
378 does not affect the steady state expression or stability of VEGF-A levels in the TMEM doorway.
379 **(Figure 3G, H)**. Both findings are consistent with the observation that tumor cell secreted CSF-1
380 does not upregulate VEGF-A expression in macrophages **(Supplementary Figure 2)**, but rather
381 controls VEGF-A secretion from macrophages, which is retained within the TMEM doorway.
382 Altogether, these results indicate that tumor cells stimulate macrophages to release VEGF-A but
383 do not induce its production within macrophages.

384

385 **Inhibition of CSF-1R reduces TMEM doorway-associated vascular opening and trans-**
386 **endothelial migration**

387 As CSF-1R signaling regulates macrophage VEGF-A secretion, and macrophage-
388 secreted VEGF-A is required for vascular opening at TMEM doorways (10), we examined the role
389 of the CSF-1R in mediating vascular opening and tumor cell intravasation at TMEM doorways *in*
390 *vivo,* as defined in **Figure 1** and previously (6). We injected tumor bearing PyMT mice *i.v.* with
391 CSF-1R blocking antibodies or IgG control antibodies, four hours prior to sacrifice, and injected
392 high molecular weight dextran (155 kDa), one hour before sacrifice. We stained the tumor tissue
393 for CD31, TMR-Dextran, and ZO-1 to examine the effects of CSF-1R inhibition on TMEM doorway
394 activity and vascular junctional integrity (**Figure 4A).** Acute inhibition of CSF-1R reduced
395 extravascular dextran (red) at TMEM doorways, indicating that TMEM doorways were less active
396 when CSF-1 signaling is inhibited **(Figure 4B)**. Vascular ZO-1, a component of endothelial tight
397 junctions that maintains vascular junction integrity, increased with inhibition of CSF-1R suggesting
398 that the endothelial junctions were less permeable upon CSF-1R inhibition **(Figure 4C)**. To

399 determine whether blockade of CSF-1 signaling and subsequent inhibition of TMEM doorway
400 opening prevented tumor cells from entering the vasculature, we collected the blood of the mice
401 during sacrifice and measured the number of circulating tumor cells (CTCs). The number of CTCs
402 were significantly reduced upon CSF-1R inhibition compared to control treated mice **(Figure 4D)**.
403 These results indicate that CSF-1R signaling is not only involved in tumor cell and macrophage
404 streaming migration, as reported before (8), but also in signaling between tumor cells,
405 macrophages, and endothelial cells, creating intravasation-associated vascular openings and
406 allowing intravasation of tumor cells, leading to CTCs.

407 To further examine the effects of blocking CSF-1R signaling on macrophage-mediated
408 transendothelial migration of tumor cells, we used our previously established *in vitro* trans-
409 endothelial migration (iTEM) assay (34). The iTEM assay mimics the conditions seen at the TMEM
410 doorway during intravasation (10, 32) and allows us to quantify the number of tumor cells that
411 cross the endothelium. We have previously shown that breast tumor cells seeded alone atop a
412 matrigel matrix and confluent endothelial monolayer cross through the endothelial cell barrier
413 poorly, but transendothelial migration is enhanced in the presence of macrophages (34, 35). As
414 shown before, tumor cells exhibited a basal level of trans-endothelial migration, which was
415 significantly increased in the presence of macrophages (**Figure 4E**). However, there was no
416 enhancement of tumor cell trans-endothelial migration in presence of macrophages when CSF-
417 1R signaling was inhibited by either a CSF-1R blocking antibody or a small molecule inhibitor of
418 CSF-1R (**Figure 4E**).

419 To further establish that CSF-1R signaling between tumor cells and macrophages was
420 important for enhancing tumor cell migration across the endothelial cell layer, we used BMMs
421 lacking CSF-1R (*Csf1r*$^{-/-}$) in the iTEM assay. We observed no increase in the transmigration of
422 tumor cells seeded with *Csf1r*$^{-/-}$ macrophages compared to tumor cells cultured without
423 macrophages; however, tumor cell transendothelial migration was enhanced when seeded with
424 macrophages expressing the CSF-1R (*Csf1r*$^{+/+}$) **(Figure 4F)**. Similarly, to establish that CSF-1

425 secreted by tumor cells specifically is responsible for the increased trans-endothelial migration,
426 and not the other TMEM doorway cells present in the iTEM assay, we knocked down CSF-1 in
427 MDA-MB-231 cells using siRNA (**Supplementary Figure 3**) and used these tumor cells in the
428 iTEM assay. We found that unlike tumor cells expressing CSF-1, tumor cells with reduced CSF-
429 1 expression did not support increased trans-endothelial migration in the presence of
430 macrophages (**Figure 4G**). Thus, inhibition of CSF-1R signaling blocked the ability of
431 macrophages to enhance tumor cell trans-endothelial migration.
432

433 **Discussion:**

434 It has been previously shown that TMEM doorway associated vascular opening (TAVO)
435 requires vascular endothelial growth factor-A (VEGF-A) produced by the TMEM doorway
436 macrophage. In particular, a TIE2^{hi}/VEGF-A^{hi} TMEM doorway-associated macrophage interacts
437 with its associated endothelial cell through secretion of VEGF-A to mediate blood vessel opening
438 by disrupting endothelial cell adherens and tight junctions (10). We have demonstrated, using
439 intravital imaging, that the vascular opening in tumors is an acute, localized, and transient event,
440 and only occurs at TMEM doorways, as opposed to VEGF-A injected into the vasculature, which
441 caused general and continuous leakage of blood contents from all blood vessels (10). We have
442 further shown that these TAVO events occur simultaneously with tumor cell intravasation, and are
443 required for tumor cell intravasation. When VEGF-A is knocked out specifically in macrophages,
444 TAVO events are blocked, as is tumor cell intravasation (10). These observations are consistent
445 with and provide a mechanism for the finding that the number of TMEM doorways measured by
446 multiplex immunohistochemistry in formalin-fixed paraffin-embedded breast cancer sections is a
447 clinically validated prognostic indicator of distant metastasis in breast cancer patients (12-14).
448 However, the signal provided by CSF-1 that triggers the secretion of VEGF-A by the TMEM
449 doorway macrophage, the most critical step for TMEM doorway opening, has remained unknown,
450 until now.

451 CSF-1 drives the differentiation of myeloid precursors to macrophages and is essential for
452 survival of macrophages (36-38). CSF-1/CSF-1R signaling is important for tissue homeostasis,
453 repair, and inflammation and acts as a chemoattractant for the recruitment, production, and
454 survival of tumor associated macrophages (TAMs) to the tumor microenvironment (39, 40). TAMs
455 promote tumor progression through stimulation of angiogenesis, secretion of IL-10, TGFβ, and
456 VEGF-A, and driving of tumor cell migration, invasion, and metastasis (41-43). As we show here,
457 VEGF-A secretion from TMEM doorway macrophages can be triggered by tumor cell derived-
458 CSF-1 binding to the CSF-1R on the macrophage (Figures 2 and 3). Given that CSF-1 signaling
459 is known to drive invasiveness and increase metastasis, unsurprisingly, increased expression of
460 CSF-1 is correlated with poor prognosis in ovarian, breast, and prostate cancer patients (44-49).
461 There is evidence of a paracrine interaction between tumor cells and macrophages, which
462 facilitates tumor cell migration toward blood vessels in breast cancer (8, 29). This interaction is
463 driven by a CSF-1/EGF paracrine loop, wherein tumor cells secrete CSF-1 (which attracts CSF-
464 1R expressing macrophages), while macrophages in turn secrete EGF (which attracts EGFR-
465 expressing tumor cells). The tumor cells respond to EGF-secreting macrophages by migrating
466 towards them and secreting more CSF-1, therefore generating a paracrine loop (8, 27, 29, 50).
467 These signaling events create a chemotactic axis in which the CSF-1/EGF signals become
468 amplified, allowing the tumor cells and macrophages to remain in close proximity with each other
469 as they migrate together as cell pairs (a process called streaming (8, 27, 29, 36)). Once the tumor
470 cells within the loop encounter a Hepatic Growth Factor (HGF) signal, which is found in a gradient
471 in the tumor microenvironment with the highest concentration near blood vessels (7), the tumor
472 cell-macrophage pairs start migrating toward the blood vessels along the HGF gradient, adding
473 directionality to the streaming cell pairs **(Figure 5A)**. Once at the blood vessels, the streaming
474 tumor cells can intravasate through active TMEM doorways, following a TAVO event (7, 10, 11).
475 The genetic or pharmacological inhibition of EGF, CSF-1, or the HGF receptor (c-Met) significantly
476 impairs streaming of both tumor cells and macrophages and blocks tumor cell dissemination in *in*

477 *vivo* breast cancer metastasis models (7, 8, 29, 50), confirming the critical role of the paracrine
478 CSF-1/EGF loop between tumor cells and macrophages, as well as the HGF gradient, in
479 metastasis.

480 Here we demonstrate that while the TMEM doorway tumor cell and macrophage remain
481 in direct and stable contact on the blood vessel (10, 13), the CSF-1 signaling persists, resulting
482 in localized macrophage secretion of VEGF-A. We found that TMEM doorway tumor cells secrete
483 CSF-1 which binds to the CSF-1R on TMEM doorway macrophages **(Figure 5B)**. We further show
484 that this event triggers localized secretion of VEGF-A by TMEM doorway macrophages and leads
485 to downstream TAVO events, where acute vascular opening within the endothelium allows tumor
486 cells to intravasate through the TMEM doorway. Previously, we have visualized and characterized
487 that the resulting CTCs can form distant metastases **(Figure 5C, D)** (10, 31, 51). In this study, we
488 demonstrate that inhibition of CSF-1R *in vitro* by either knocking out CSF-1R in macrophages or
489 adding a blocking antibody decreased macrophage release of VEGF-A, and transendothelial
490 migration of tumor cells, an *in vitro* measure of intravasation capability. *In vivo*, acute treatment
491 of tumor bearing mice with a CSF-1R blocking antibody significantly increased vascular tight
492 junction stability, decreased TMEM doorway activity and TAVO events, as well as formation of
493 CTCs. We did not detect a difference in VEGF-A expression around the TMEM doorway when a
494 CSF-1R blocking antibody was used *in vivo* (Figure 3G, 3H). Given that this is a relatively short-
495 term experiment, sacrificing mice four hours after treatment, and the TAVO is a rare event, we
496 expect that detecting a change in VEGF-A expression within the TMEM doorways is not possible
497 in this limited timeframe. Further, we have found that CSF-1 signaling does not increase
498 expression of VEGF-A in the TMEM doorway macrophage, but rather triggers its local secretion,
499 where VEGF-A binds to and signals to the nearby TMEM doorway endothelial cell, while
500 remaining within the TMEM doorway.

501 The importance of this study beyond the primary tumor is emphasized by the finding that
502 TMEM doorways are found not only in invasive ductal breast carcinomas, but also in metastatic

503 foci in lymph nodes (18, 19) and lungs (6). We and others have found that secondary metastases
504 can seed tertiary metastases (1-4), and the presence of TMEM doorways at secondary sites may
505 perpetuate metastatic dissemination **(Figure 5D)** even after removal of the primary tumor.
506 Importantly, blocking the function of TMEM doorways could not only prevent the dissemination of
507 cancer cells from primary tumors, but also prevent re-dissemination of tumor cells from metastatic
508 sites, which may occur after the resection of primary tumors (10, 11, 52, 53). Therefore, even if
509 the tumors are highly metastatic, we may be able to increase patient survival or quality of life, or
510 both, by blocking TMEM doorway function systemically, which would lessen overall metastatic
511 burden. Inhibition of both Tie2 and CSF-1 signaling to prevent TAVO events (10, 31), along with
512 standard of care therapies, might be an effective way to prevent re-dissemination from both
513 primary and metastatic tumor sites, and allow for better patient survival.

514 Recent preclinical studies targeting CSF-1/CSF-1R have yielded promising results in
515 several tumor models. A monoclonal antibody targeting CSF-1R depleted TAMs and increased
516 the $CD8^+/CD4^+$ T cell ratio, leading to decreased primary tumor burden and decreased metastasis
517 in mouse models of colorectal cancer and fibrosarcoma (54). Another recent study investigating
518 breast and colon carcinoma models found that CSF-1/CSF-1R signaling inhibition stimulated the
519 expansion of neo-epitope specific T cells and promoted the development of an immune-
520 permissive TME (55). So far, the FDA has approved one CSF-1R inhibitor for patients with
521 tenosynovial giant cell tumors, a tumor type characterized by chromosomal translocations of the
522 CSF-1 gene, leading to aberrant CSF-1 expression (56, 57). Despite the promising preclinical
523 studies using CSF-1/CSF-1R inhibitors in combination with chemotherapy, immunotherapy, or
524 radiotherapy, phase II clinical trials have not yielded the same anti-tumor efficacies (58-64). In
525 patients with advanced triple negative breast cancer, the combination of a CSF-1 monoclonal
526 antibody with gemcitabine and carboplatin showed comparable anti-tumor activity compared to
527 gemcitabine and carboplatin alone (65). In another phase Ib/II study, patients with advanced
528 pancreatic ductal carcinoma, colorectal cancer, or non-small cell lung cancer were treated with a

529 CSF-1R monoclonal antibody plus anti-PD-1 therapy; however, minimal anti-tumor activity was
530 observed (62). In these studies, investigators were expecting to observe an enhancement in
531 intratumoral infiltration of $CD8^+/CD4^+$ T cells and TAM depletion, given the role that CSF-1
532 signaling plays in creating an immune suppressive environment and promoting recruitment,
533 survival and differentiation of macrophages. Taking into consideration our findings that CSF-1
534 signaling is critical for the recruitment of tumor cell-macrophage pairs to the blood vessels in the
535 primary tumor (8, 27, 29, 50), the transient opening of the blood vessels at TMEM doorways
536 (Figure 4B), and intravasation of tumor cells at TMEM doorways (Figure 4D), we expect that
537 treating patients with less advanced disease would be efficacious in preventing metastatic
538 disease or reducing metastatic burden, though not necessarily in preventing primary tumor
539 growth. Additionally, given our findings that TMEM doorway scores are predictive of distant
540 metastasis in subsets of breast cancer patients (12-14), we contend that selecting the breast
541 cancer patients meeting the criteria for predictive metastatic disease for the clinical trials would
542 show increased success in improving patient outcomes. Our study provides evidence that the
543 mechanism through which CSF-1R inhibition can prevent metastasis is not only by macrophage
544 depletion, but also by blocking CSF-1/CSF-1R paracrine signaling between tumor cells and
545 macrophages leading to inhibition in tumor cell intravasation in the primary tumor.

546 We have previously shown in mice that transient, short-term blockade of VEGF-A
547 expression in macrophages is effective in inhibiting TMEM doorway activity, TAVO events, and
548 formation of CTCs (10). However, if patients are treated with anti-angiogenic therapies targeting
549 VEGF-A (e.g., bevacizumab and other VEGF-A inhibitors) they eventually develop therapeutic
550 resistance (66). One mechanism of tumor resistance or recurrence following anti-angiogenic
551 therapy in patients is attributed to the increased recruitment and infiltration of Tie2-expressing
552 macrophages into the tumor in response to apoptosis, necrosis, and hypoxia after vascular
553 regression (66). Additionally, the ligand for Tie2, Ang2, is upregulated in response to hypoxic
554 conditions. Tie2-Ang2 signaling can function in a similar manner to VEGF-A signaling to promote

555 tumor angiogenesis, bypassing VEGF-A inhibition, and even being enhanced by such inhibition.
556 As such, Tie2 is an attractive pharmacological target for the suppression of tumor angiogenesis
557 and tumor cell dissemination. We have found that TMEM doorway macrophages are also
558 characterized by expression of Tie2 (10) and that a selective inhibitor of Tie2, rebastinib, inhibits
559 TMEM doorway activity, formation of CTCs, and metastasis in several mouse models of
560 metastasis and patient derived xenografts (32). The mechanism of how Tie2 contributes to
561 signaling between the TMEM doorway cells to mediate the TAVO events is still unclear and
562 warrants further investigation. Uncovering the complete mechanism of TMEM doorway opening
563 in primary and secondary sites is critical. We expect that inhibiting TAVO events, potentially by
564 targeting both CSF-1 and Tie2 signaling, will improve our ability to increase the survival of both
565 patients with metastatic disease and patients who are likely to develop metastatic disease.
566

567 **Acknowledgments:**
568 This work was supported by the NCI grants (R01 CA255153, PPG CA257885, R01 CA240646,
569 F32 CA243350), SIG OD019961, the Gruss-Lipper Biophotonics Center, the Integrated Imaging
570 Program, the Integrated Imaging Program for Cancer Research, The Evelyn Gruss-Lipper
571 Charitable Foundation, and The Helen & Irving Spatz Family Foundation. We would like to thank
572 the Analytical Imaging Facility at Albert Einstein College of Medicine for imaging support.
573

574 **Author contributions:**
575 Conceptualization: CRS, ASH, MHO, JSC
576 Methodology: CRS, ASH, XY,
577 Formal Analysis: CRS, CLD, XY, VPS, DE, MHO
578 Software: XY, DE
579 Investigation: CRS, CLD, XC, YL, ASH, YW, VPS
580 Resources: ERS, DC, DE

581 Writing: CRS, CLD, ASH, ERS, MHO, JSC

582 Funding Acquisition: CLD, DE, MHO, JSC

583 Supervision: ERS, JCM, DE, MHO, JSC

584

585 **Competing interests:** The authors declare no competing financial interests.

586

587 **Data availability statement:** Data sharing is not applicable to this article as no datasets were

588 generated or analyzed during the current study.

589

590 **References:**

591 1. Borriello L, Condeelis J, Entenberg D, Oktay MH. Breast Cancer Cell Re-Dissemination from Lung

592 Metastases-A Mechanism for Enhancing Metastatic Burden. J Clin Med. 2021;10(11).

593 2. Kim MY, Oskarsson T, Acharyya S, Nguyen DX, Zhang XH, Norton L, et al. Tumor self-seeding by

594 circulating cancer cells. Cell. 2009;139(7):1315-26.

595 3. Chaffer CL, Weinberg RA. A perspective on cancer cell metastasis. Science. 2011;331(6024):1559-

596 64.

597 4. Zhang W, Bado IL, Hu J, Wan YW, Wu L, Wang H, et al. The bone microenvironment invigorates

598 metastatic seeds for further dissemination. Cell. 2021;184(9):2471-86.e20.

599 5. Quail DF, Joyce JA. Microenvironmental regulation of tumor progression and metastasis. Nat Med.

600 2013;19(11):1423-37.

601 6. Condeelis J, Pollard JW. Macrophages: obligate partners for tumor cell migration, invasion, and

602 metastasis. Cell. 2006;124(2):263-6.

603 7. Leung E, Xue A, Wang Y, Rougerie P, Sharma VP, Eddy R, et al. Blood vessel endothelium-
604 directed tumor cell streaming in breast tumors requires the HGF/C-Met signaling pathway. Oncogene.
605 2017;36(19):2680-92.
606 8. Wyckoff J, Wang W, Lin EY, Wang Y, Pixley F, Stanley ER, et al. A paracrine loop between tumor
607 cells and macrophages is required for tumor cell migration in mammary tumors. Cancer Res.
608 2004;64(19):7022-9.
609 9. Borriello L, Karagiannis GS, Duran CL, Coste A, Oktay MH, Entenberg D, et al. The role of the
610 tumor microenvironment in tumor cell intravasation and dissemination. Eur J Cell Biol.
611 2020;99(6):151098.
612 10. Harney AS, Arwert EN, Entenberg D, Wang Y, Guo P, Qian BZ, et al. Real-Time Imaging Reveals
613 Local, Transient Vascular Permeability, and Tumor Cell Intravasation Stimulated by TIE2hi Macrophage-
614 Derived VEGFA. Cancer Discov. 2015;5(9):932-43.
615 11. Wyckoff JB, Wang Y, Lin EY, Li JF, Goswami S, Stanley ER, et al. Direct visualization of
616 macrophage-assisted tumor cell intravasation in mammary tumors. Cancer Res. 2007;67(6):2649-56.
617 12. Sparano JA, Gray R, Oktay MH, Entenberg D, Rohan T, Xue X, et al. A metastasis biomarker
618 (MetaSite Breast Score) is associated with distant recurrence in hormone receptor-positive, HER2-
619 negative early-stage breast cancer. NPJ Breast Cancer. 2017;3:42.
620 13. Robinson BD, Sica GL, Liu YF, Rohan TE, Gertler FB, Condeelis JS, et al. Tumor microenvironment
621 of metastasis in human breast carcinoma: a potential prognostic marker linked to hematogenous
622 dissemination. Clinical Cancer Research 2009;15(7):2433-41.
623 14. Rohan TE, Xue X, Lin HM, D'Alfonso TM, Ginter PS, Oktay MH, et al. Tumor microenvironment of
624 metastasis and risk of distant metastasis of breast cancer. J Natl Cancer Inst. 2014;106(8).

625 15. Kim G, Karadal-Ferrena B, Qin J, Sharma VP, Oktay IS, Lin Y, et al. Racial disparity in tumor
626 microenvironment and distant recurrence in residual breast cancer after neoadjuvant chemotherapy.
627 NPJ Breast Cancer. 2023;9(1):52.
628 16. Kim G, Pastoriza JM, Qin J, Lin J, Karagiannis GS, Condeelis JS, et al. Racial disparity in distant
629 recurrence-free survival in patients with localized breast cancer: A pooled analysis of National Surgical
630 Adjuvant Breast and Bowel Project trials. Cancer. 2022;128(14):2728-35.
631 17. Albain KS, de la Garza Salazar J, Pienkowski T, Aapro M, Bergh J, Caleffi M, et al. Reducing the
632 global breast cancer burden: the importance of patterns of care research. Clin Breast Cancer.
633 2005;6(5):412-20.
634 18. Ginter PS, Karagiannis GS, Entenberg D, Lin Y, Condeelis J, Jones JG, et al. Tumor
635 Microenvironment of Metastasis (TMEM) Doorways Are Restricted to the Blood Vessel Endothelium in
636 Both Primary Breast Cancers and Their Lymph Node Metastases. Cancers (Basel). 2019;11(10):1507.
637 19. Coste A, Karagiannis GS, Wang Y, Xue EA, Lin Y, Skobe M, et al. Hematogenous Dissemination of
638 Breast Cancer Cells From Lymph Nodes Is Mediated by Tumor MicroEnvironment of Metastasis
639 Doorways. Front Oncol. 2020;10:571100.
640 20. Entenberg D, Pastoriza JM, Oktay MH, Voiculescu S, Wang Y, Sosa MS, et al. Time-lapsed, large-
641 volume, high-resolution intravital imaging for tissue-wide analysis of single cell dynamics. Methods.
642 2017;128:65-77.
643 21. Linde N, Casanova-Acebes M, Sosa MS, Mortha A, Rahman A, Farias E, et al. Macrophages
644 orchestrate breast cancer early dissemination and metastasis. Nat Commun. 2018;9(1):21.
645 22. Harney AS, Wang Y, Condeelis JS, Entenberg D. Extended Time-lapse Intravital Imaging of Real-
646 time Multicellular Dynamics in the Tumor Microenvironment. J Vis Exp. 2016(112):e54042.
647 23. Karagiannis GS, Goswami S, Jones JG, Oktay MH, Condeelis JS. Signatures of breast cancer
648 metastasis at a glance. J Cell Sci. 2016;129(9):1751-8.

649 24. Entenberg D, Voiculescu S, Guo P, Borriello L, Wang Y, Karagiannis GS, et al. A permanent
650 window for the murine lung enables high-resolution imaging of cancer metastasis. Nat Methods.
651 2018;15(1):73-80.
652 25. Curry JM, Eubank TD, Roberts RD, Wang Y, Pore N, Maity A, et al. M-CSF signals through the
653 MAPK/ERK pathway via Sp1 to induce VEGF production and induces angiogenesis in vivo. PLoS One.
654 2008;3(10):e3405.
655 26. Eubank TD, Galloway M, Montague CM, Waldman WJ, Marsh CB. M-CSF induces vascular
656 endothelial growth factor production and angiogenic activity from human monocytes. J Immunol.
657 2003;171(5):2637-43.
658 27. Patsialou A, Wyckoff J, Wang Y, Goswami S, Stanley ER, Condeelis JS. Invasion of human breast
659 cancer cells in vivo requires both paracrine and autocrine loops involving the colony-stimulating factor-1
660 receptor. Cancer Res. 2009;69(24):9498-506.
661 28. Hernandez L, Smirnova T, Kedrin D, Wyckoff J, Zhu L, Stanley ER, et al. The EGF/CSF-1 paracrine
662 invasion loop can be triggered by heregulin beta1 and CXCL12. Cancer Res. 2009;69(7):3221-7.
663 29. Goswami S, Sahai E, Wyckoff JB, Cammer M, Cox D, Pixley FJ, et al. Macrophages promote the
664 invasion of breast carcinoma cells via a colony-stimulating factor-1/epidermal growth factor paracrine
665 loop. Cancer Res. 2005;65(12):5278-83.
666 30. Karagiannis GS, Pastoriza JM, Borriello L, Jafari R, Coste A, Condeelis JS, et al. Assessing Tumor
667 Microenvironment of Metastasis Doorway-Mediated Vascular Permeability Associated with Cancer Cell
668 Dissemination using Intravital Imaging and Fixed Tissue Analysis. J Vis Exp. 2019(148).
669 31. Karagiannis GS, Pastoriza JM, Wang Y, Harney AS, Entenberg D, Pignatelli J, et al. Neoadjuvant
670 chemotherapy induces breast cancer metastasis through a TMEM-mediated mechanism. Sci Transl Med.
671 2017;9(397).

672 32. Harney AS, Karagiannis GS, Pignatelli J, Smith BD, Kadioglu E, Wise SC, et al. The Selective Tie2
673 Inhibitor Rebastinib Blocks Recruitment and Function of Tie2(Hi) Macrophages in Breast Cancer and
674 Pancreatic Neuroendocrine Tumors. Mol Cancer Ther. 2017;16(11):2486-501.
675 33. Yu W, Chen J, Xiong Y, Pixley FJ, Dai XM, Yeung YG, et al. CSF-1 receptor structure/function in
676 MacCsf1r-/- macrophages: regulation of proliferation, differentiation, and morphology. J Leukoc Biol.
677 2008;84(3):852-63.
678 34. Roh-Johnson M, Bravo-Cordero JJ, Patsialou A, Sharma VP, Guo P, Liu H, et al. Macrophage
679 contact induces RhoA GTPase signaling to trigger tumor cell intravasation. Oncogene. 2014;33(33):4203-
680 12.
681 35. Pignatelli J, Bravo-Cordero JJ, Roh-Johnson M, Gandhi SJ, Wang Y, Chen X, et al. Macrophage-
682 dependent tumor cell transendothelial migration is mediated by Notch1/MenaINV-initiated
683 invadopodium formation. Sci Rep. 2016;6:37874.
684 36. Hume DA, MacDonald KP. Therapeutic applications of macrophage colony-stimulating factor-1
685 (CSF-1) and antagonists of CSF-1 receptor (CSF-1R) signaling. Blood. 2012;119(8):1810-20.
686 37. Chitu V, Stanley ER. Colony-stimulating factor-1 in immunity and inflammation. Curr Opin
687 Immunol. 2006;18(1):39-48.
688 38. Stanley ER, Chitu V. CSF-1 receptor signaling in myeloid cells. Cold Spring Harb Perspect Biol.
689 2014;6(6).
690 39. Lin W, Xu D, Austin CD, Caplazi P, Senger K, Sun Y, et al. Function of CSF1 and IL34 in
691 Macrophage Homeostasis, Inflammation, and Cancer. Front Immunol. 2019;10:2019.
692 40. da Silva SD, Marchi FA, Su J, Yang L, Valverde L, Hier J, et al. Co-Overexpression of TWIST1-CSF1
693 Is a Common Event in Metastatic Oral Cancer and Drives Biologically Aggressive Phenotype. Cancers
694 (Basel). 2021;13(1).

695 41. Jayasingam SD, Citartan M, Thang TH, Mat Zin AA, Ang KC, Ch'ng ES. Evaluating the Polarization
696 of Tumor-Associated Macrophages Into M1 and M2 Phenotypes in Human Cancer Tissue: Technicalities
697 and Challenges in Routine Clinical Practice. Front Oncol. 2019;9:1512.
698 42. Wynn TA, Chawla A, Pollard JW. Macrophage biology in development, homeostasis and disease.
699 Nature. 2013;496(7446):445-55.
700 43. Biswas SK, Mantovani A. Macrophage plasticity and interaction with lymphocyte subsets: cancer
701 as a paradigm. Nat Immunol. 2010;11(10):889-96.
702 44. Behnes CL, Bremmer F, Hemmerlein B, Strauss A, Strobel P, Radzun HJ. Tumor-associated
703 macrophages are involved in tumor progression in papillary renal cell carcinoma. Virchows Arch.
704 2014;464(2):191-6.
705 45. Kacinski BM. CSF-1 and its receptor in ovarian, endometrial and breast cancer. Ann Med.
706 1995;27(1):79-85.
707 46. Kwon OJ, Zhang B, Jia D, Zhang L, Wei X, Zhou Z, et al. Elevated expression of the colony-
708 stimulating factor 1 (CSF1) induces prostatic intraepithelial neoplasia dependent of epithelial-Gp130.
709 Oncogene. 2022;41(9):1309-23.
710 47. Mroczko B, Groblewska M, Wereszczynska-Siemiatkowska U, Okulczyk B, Kedra B, Laszewicz W,
711 et al. Serum macrophage-colony stimulating factor levels in colorectal cancer patients correlate with
712 lymph node metastasis and poor prognosis. Clin Chim Acta. 2007;380(1-2):208-12.
713 48. Smith HO, Anderson PS, Kuo DY, Goldberg GL, DeVictoria CL, Boocock CA, et al. The role of
714 colony-stimulating factor 1 and its receptor in the etiopathogenesis of endometrial adenocarcinoma.
715 Clin Cancer Res. 1995;1(3):313-25.
716 49. Yang L, Wu Q, Xu L, Zhang W, Zhu Y, Liu H, et al. Increased expression of colony stimulating
717 factor-1 is a predictor of poor prognosis in patients with clear-cell renal cell carcinoma. BMC Cancer.
718 2015;15:67.

719 50. Patsialou A, Wang Y, Pignatelli J, Chen X, Entenberg D, Oktay M, et al. Autocrine CSF1R signaling
720 mediates switching between invasion and proliferation downstream of TGFbeta in claudin-low breast
721 tumor cells. Oncogene. 2015;34(21):2721-31.
722 51. Sharma VP, Tang B, Wang Y, Duran CL, Karagiannis GS, Xue EA, et al. Live tumor imaging shows
723 macrophage induction and TMEM-mediated enrichment of cancer stem cells during metastatic
724 dissemination. Nat Commun. 2021;12(1):7300.
725 52. Wyckoff J, Gligorijevic B, Entenberg D, Segall J, Condeelis J. High-resolution multiphoton imaging
726 of tumors in vivo. Cold Spring Harb Protoc. 2011;2011(10):1167-84.
727 53. Dovas A, Patsialou A, Harney AS, Condeelis J, Cox D. Imaging interactions between macrophages
728 and tumour cells that are involved in metastasis in vivo and in vitro. J Microsc. 2013;251(3):261-9.
729 54. Ries CH, Cannarile MA, Hoves S, Benz J, Wartha K, Runza V, et al. Targeting tumor-associated
730 macrophages with anti-CSF-1R antibody reveals a strategy for cancer therapy. Cancer Cell.
731 2014;25(6):846-59.
732 55. Maldonado MDM, Schlom J, Hamilton DH. Blockade of tumor-derived colony-stimulating factor
733 1 (CSF1) promotes an immune-permissive tumor microenvironment. Cancer Immunol Immunother.
734 2023;72(10):3349-62.
735 56. Benner B, Good L, Quiroga D, Schultz TE, Kassem M, Carson WE, et al. Pexidartinib, a Novel Small
736 Molecule CSF-1R Inhibitor in Use for Tenosynovial Giant Cell Tumor: A Systematic Review of Pre-Clinical
737 and Clinical Development. Drug Des Devel Ther. 2020;14:1693-704.
738 57. West RB, Rubin BP, Miller MA, Subramanian S, Kaygusuz G, Montgomery K, et al. A landscape
739 effect in tenosynovial giant-cell tumor from activation of CSF1 expression by a translocation in a
740 minority of tumor cells. Proc Natl Acad Sci U S A. 2006;103(3):690-5.
741 58. Neubert NJ, Schmittnaegel M, Bordry N, Nassiri S, Wald N, Martignier C, et al. T cell-induced
742 CSF1 promotes melanoma resistance to PD1 blockade. Sci Transl Med. 2018;10(436).

743 59. Zhu Y, Knolhoff BL, Meyer MA, Nywening TM, West BL, Luo J, et al. CSF1/CSF1R blockade
744 reprograms tumor-infiltrating macrophages and improves response to T-cell checkpoint immunotherapy
745 in pancreatic cancer models. Cancer Res. 2014;74(18):5057-69.
746 60. Holmgaard RB, Brachfeld A, Gasmi B, Jones DR, Mattar M, Doman T, et al. Timing of CSF-1/CSF-
747 1R signaling blockade is critical to improving responses to CTLA-4 based immunotherapy.
748 Oncoimmunology. 2016;5(7):e1151595.
749 61. Falchook GS, Peeters M, Rottey S, Dirix LY, Obermannova R, Cohen JE, et al. A phase 1a/1b trial
750 of CSF-1R inhibitor LY3022855 in combination with durvalumab or tremelimumab in patients with
751 advanced solid tumors. Invest New Drugs. 2021;39(5):1284-97.
752 62. Razak AR, Cleary JM, Moreno V, Boyer M, Calvo Aller E, Edenfield W, et al. Safety and efficacy of
753 AMG 820, an anti-colony-stimulating factor 1 receptor antibody, in combination with pembrolizumab in
754 adults with advanced solid tumors. J Immunother Cancer. 2020;8(2).
755 63. Carleton M, Powers J, Phillips P, Beg MS, Lee JJ, Rahma OE, et al. Pharmacodynamics (PD) and
756 genomic profiling of pts treated with cabiralizumab (cabira) plus nivolumab (NIVO) provide evidence of
757 on-target tumor immune modulations and support future clinical applications. J Clin Oncol. 2018;36(15).
758 64. Calvo A, Joensuu H, Sebastian M, Naing A, Bang YJ, Martin M, et al. Phase Ib/II study of
759 lacnotuzumab (MCS110) combined with spartalizumab (PDR001) in patients (pts) with advanced tumors.
760 J Clin Oncol. 2018;36(15).
761 65. Kuemmel S, Campone M, Loirat D, Lopez RL, Beck JT, De Laurentiis M, et al. A Randomized Phase
762 II Study of Anti-CSF1 Monoclonal Antibody Lacnotuzumab (MCS110) Combined with Gemcitabine and
763 Carboplatin in Advanced Triple-Negative Breast Cancer. Clin Cancer Res. 2022;28(1):106-15.
764 66. Bergers G, Hanahan D. Modes of resistance to anti-angiogenic therapy. Nat Rev Cancer.
765 2008;8(8):592-603.

766 67. Morgan C, Pollard JW, Stanley ER. Isolation and characterization of a cloned growth factor
767 dependent macrophage cell line, BAC1.2F5. J Cell Physiol. 1987;130(3):420-7.
768 68. Guy CT CR, Muller WJ. Induction of mammary tumors by expression of polyomavirus middle T
769 oncogene: a transgenic mouse model for metastatic disease. Molecular and cellular biology. 1992;12(3).
770 69. Schneider CA, Rasband WS, Eliceiri KW. NIH Image to ImageJ: 25 years of image analysis. Nat
771 Methods. 2012;9(7):671-5.
772 70. Pignatelli J, Goswami S, Jones JG, Rohan TE, Pieri E, Chen X, et al. Invasive breast carcinoma cells
773 from patients exhibit MenaINV- and macrophage-dependent transendothelial migration. Sci Signal.
774 2014;7(353):ra112.
775 71. Cabrera RM, Mao SPH, Surve CR, Condeelis JS, Segall JE. A novel neuregulin - jagged1 paracrine
776 loop in breast cancer transendothelial migration. Breast Cancer Res. 2018;20(1):24.

777 **Figure Legends:**

778 **Figure 1. TMEM doorway tumor cells show increased CSF-1 levels at active TMEM**
779 **doorways. A)** Cartoon denoting the identification of parameters used for analysis of CSF-1 levels
780 in TMEM doorway tumor cells (TTCs) and TMEM doorway function. The three cells composing
781 the TMEM doorway are indicated by the yellow triangle connecting the TMEM doorway
782 macrophage (TM), the TMEM doorway endothelial cell (TEC) and the TTC. Intravascular dextran
783 is in the lumen of blood vessel, extravascular dextran is outside the lumen of blood vessel, and
784 CSF-1 is directly measured in the TTC. Figure created with BioRender.com. **B)** Panel shows
785 inactive and active TMEM doorways, visualized by immunohistochemistry (IHC) staining for
786 Mena, Iba-1, and endomucin. The three cells of the TMEM doorway (contained in black circle,
787 with the three cells forming the TMEM doorway indicated with the yellow triangle) are the TMEM
788 doorway endothelial cell (TEC, endomucin stained in blue, circled in white), TMEM doorway
789 macrophage (TM, Iba1 stained in brown, circled in teal), and TMEM doorway tumor cell (TTC,
790 Mena stained in pink, and circled in pink) and black arrows indicate where the cells are localized
791 within the TMEM doorway. TMEM doorways were identified using automated analysis by
792 VisioPharm identifying three adjacent immuno-histochemical stains. **C)** The sequential tissue
793 sections after the IHC in (B) were stained with immunofluorescence (IF) with antibodies against
794 endomucin (white), dextran (green), CSF-1 (red), and nuclear stain DAPI (blue). The two
795 sequential sections from 1B and 1C were aligned and the same TMEM doorways were matched
796 between the two sections, as indicated by the black circle in the IHC panel (1B) and white circle
797 in the IF panels (1C) showing the same TMEM doorway after alignment. The left panels
798 demonstrate the association of CSF-1 level in the TMEM doorway tumor cell (TTC) with TMEM
799 doorway activity. The middle panel shows the extravascular signal for dextran as a green mask
800 and the endomucin stain as a white mask, where thresholded, positive signal for these stains was
801 converted into a binary mask. Active versus inactive TMEM doorways were distinguished by the
802 presence of extravascular dextran staining non-overlapping with the endomucin stain, which

803 indicates that the vessel had a TMEM doorway-associated vascular opening (TAVO). Scale
804 bars=20μm. **D)** Immunofluorescence measurement of CSF-1 levels in TMEM doorway tumor cells
805 in active and inactive TMEM doorways. TMEM doorways were identified in the IF-stained sections
806 as described above. Active TMEM doorways were identified by the presence of extravascular
807 dextran which is not present in inactive TMEM doorways (see panel C). Next, tumor cells were
808 identified using the Mena positive cells at TMEM doorway (panel 1B, IHC stain). The level of CSF-
809 1 in the TMEM doorway tumor cells was measured in both active and inactive TMEM doorways
810 using Visiopharm. n= 12 mice. ****$P < 0.0001$ analyzed by Student's *t*-test.

811 **Figure 2. TMEM doorway macrophages secrete VEGF-A in response to CSF-1 and tumor**
812 **cells secrete CSF-1. A)** VEGF-A ELISA of conditioned media obtained from BAC1.2F5
813 macrophages (Mϕ) treated with or without CSF-1 (3000 units/mL) for the times indicated. VEGF-
814 A is indicated as concentration (pg/ml) of secreted protein. n=3 individual experiments done in
815 duplicate, **p<0.01, by two-way ANOVA. **B)** CSF-1 ELISA of conditioned media obtained from
816 MDA-MB 231 tumor cells (TCs). TCs were cultured for 24 hours in serum-free media and the
817 concentration of CSF-1 (pg/mL) secreted by the TCs measured in the tumor cell conditioned
818 media by ELISA. Control is media not exposed to tumor cells but treated in the same way as the
819 cells. n=3 individual experiments done in duplicate. ****p<0.0001 by Student's *t*-test. **C)**
820 Immunofluorescence staining of serial PyMT tumor sections stained for CSF-1R (green),
821 vasculature (CD31, magenta), macrophages (top: CD68, white; bottom: CD206, red) and DAPI
822 (blue). The TMEM doorway is indicated with the yellow arrow, with each point of the triangle
823 identifying each cell in the doorway, as described in Figure 1 (10). TMEM doorway cells are
824 indicated with white arrows: endothelial cell (TEC, white circle); TMEM doorway macrophage
825 (TM, blue circle); and TMEM doorway tumor cell (TTC, pink circle). Scale bar 30 μm. **D)**
826 Quantification of the percent of $CD68^+$ TMEM doorway macrophages and $CD68^+/CD206^+$
827 macrophages which stain positively for CSF-1R (n = 6).

828 **Figure 3. Tumor cell secreted CSF-1 increases CSF-1R dependent macrophage VEGF-A**
829 **secretion. A)** VEGF-A ELISA of conditioned media obtained from BAC1.2F5 macrophages co-
830 cultured with MDA-MB-231 tumor cells treated with control antibody (ctrl Ab), CSF-1R blocking
831 Ab or CSF-1R inhibitor (GW2580), denoted as concentration (pg/mL) of secreted protein. n=3
832 individual experiments performed in duplicate, *p<0.05, ***p<0.001, ****p<0.0001 analyzed by
833 two-way ANOVA. **B)** ELISA determination of VEGF-A (pg/mL) in medium obtained from
834 BAC1.2F5 macrophages cultured in medium conditioned by MDA-MB-231 tumor cells (Tumor
835 Cell CM) and treated with control Ab, CSF-1R blocking Ab (CSF-1R Ab) or CSF-1R inhibitor
836 (GW2580). n=3 individual experiments performed in duplicate, ***p<0.001, ****p<0.0001 analyzed
837 by two-way ANOVA. **C)** ELISA determination of VEGF-A (pg/mL) in medium conditioned y bone
838 marrow macrophage (BMMs) either expressing (*Csf1r*$^{+/+}$) or lacking (*Csf1r*$^{-/-}$) CSF-1R co-cultured
839 with MDA-MB-231 tumor cells for the times indicated. n=3 individual experiments done in
840 duplicate, ****p<0.0001 analyzed by two-way ANOVA. **D)** ELISA determination of VEGF-A
841 (pg/mL) in medium from *Csf1r*$^{+/+}$ or *Csf1r*$^{-/-}$ BMMs cultured in MDA-MB-231 tumor cell conditioned
842 medium (Tumor Cell CM) for the times indicated. n=3 individual experiments done in duplicate,
843 ****p<0.0001 analyzed by two-way ANOVA. **E)** BAC1.2F5 macrophages, labelled with
844 CellTracker™ Green, were co-cultured with or without MDA-MB-231 tumor cells (TC), labelled
845 with CellTracker™ Red, and treated with either control or CSF-1R blocking antibodies for 48
846 hours. Cells were fixed, permeabilized and stained for VEGF-A. Macrophages were identified by
847 the CellTracker Green label and only images of macrophages are shown. Heat map scale to right
848 shows intensity of VEGF-A staining. Scale bar 5 μm. **F)** Quantitation of the VEGF-A fluorescence
849 intensity in macrophages in (E). The amount of VEGF-A in the macrophage was quantified using
850 ImageJ, as described in the methods section. n=3. *p<0.05, **p<0.01, analyzed by one-way
851 ANOVA. **G, H)** Immuno-staining and quantification of VEGF-A intensity around TMEM doorways,
852 obtained from PyMT mice treated with control antibody (ctrl Ab) or CSF-1R blocking Ab.
853 Sequential tumor sections derived from PyMT tumors were stained by immunofluorescence

854 (VEGF-A, Iba-1) and IHC (TMEM doorways-Mena, Iba-1, endomucin). TMEM doorways were
855 identified as described in figure 1A. The circle in the IHC (black) and IF (white) panels show the
856 same TMEM doorways obtained from the alignment of serial sections, and the three cells making
857 up the TMEM doorway are pointed out with the yellow triangle in each panel. TMEM doorways
858 are outlined in the circle with the endothelial cell (TE, blue stain, white circle), macrophage (TM,
859 brown stain, teal circle) and TMEM doorway tumor cell (TTC, pink stain, pink circle) indicated with
860 arrows. Next, the two sequential sections were aligned and TMEM doorway was identified in the
861 IF-stained section. The immunofluorescence intensity of VEGF-A expression (green stain) in the
862 identified TMEM doorway ROIs was measured and plotted here. N=analysis of images obtained
863 from tissue sections from individual 11 mice, Scale bar 20 μm, not significant, analyzed by
864 Student's *t*-test.
865
866 **Figure 4. Inhibition of CSF-1R signaling reduces TAVO and trans-endothelial migration. A)**
867 IF staining of tumor tissue from mice treated with control Ab or CSF-1R Ab were stained for CD31
868 (green), TMR-dextran (red), and ZO-1 (magenta). Right panel shows increased magnification of
869 yellow box from middle panel to demonstrate overlap between CD31 and ZO-1 stains
870 (merge/overlap indicated with white signal, and pointed out with white arrows). **B)** Quantification
871 of extravascular 155 kDa dextran-TMR. *p<0.05. **C**) Vascular ZO-1 *p<0.05, and **D**) circulating
872 tumor cells for mice treated with control Ab or CSF-1R blocking Ab in A). *p<0.05, analyzed by
873 Student's *t*-test. (B, C, D, *n* = 8) **E)** Quantitation of subluminal to luminal trans-endothelial
874 migration (iTEM activity, which is a measure of number of intravasating cells in the intravasation
875 direction) of MDA-MB-231 cells plated on the confluent and sealed endothelium either alone or
876 with BAC1.2F5 macrophages. Tumor cells were treated with control antibody (ctrl Ab & DMSO),
877 CSF-1R blocking Ab (CSF-1R Ab) or CSF-1R inhibitor (GW2580). Tumor cells were labelled with
878 CellTracker™ green which allowed us to identify and quantify the cells crossing. The number of
879 MDA-MB-231 cells which crossed the endothelium were imaged using a confocal microscope and

880 quantified using ImageJ software. n=3, *p<0.05 analyzed by one-way ANOVA. **F)** Quantitation of
881 iTEM activity of MDA-MB-231 cells plated on the endothelium alone or with BMMs expressing or
882 lacking CSF-1R expression. Tumor cells were labelled with CellTracker™ green which allowed
883 us to identify and quantify the cells crossing. The number of MDA-MB-231 cells which crossed
884 the endothelium were imaged using a confocal microscope and quantified using ImageJ software.
885 N=3, ***p< 0.001 analyzed by one-way ANOVA. **G)** Quantitation of iTEM activity of MDA-MB-231
886 cells transfected with either control siRNA or two different siRNAs targeting CSF-1 (#1, #2).
887 Transfected cells were plated on the endothelium either alone or with BAC1.2F5 macrophages.
888 Tumor cells were labelled with CellTracker™ green which allowed us to identify and quantify the
889 cells crossing. The number of MDA-MB-231 cells which crossed the endothelium were imaged
890 using a confocal microscope and quantified using ImageJ software. n=3, **p<0.01, ***p< 0.001
891 analyzed by one-way ANOVA.
892
893 **Figure 5. Model of CSF-1-induced TMEM doorway opening and release of CTCs into the**
894 **blood stream. A)** In the primary tumor, macrophages and tumor cells exhibit a CSF-1/EGF
895 paracrine interaction between tumor cells and macrophages which facilitates tumor cell migration
896 toward blood vessels in breast cancer. Tumor cells secrete CSF-1 which attracts CSF-1R
897 expressing macrophages, which in turn secrete EGF, increasing the migration of EGFR-
898 expressing tumor cells. The tumor cells within the loop encounter an HGF signal found in a
899 gradient in the tumor microenvironment with the highest concentration near blood vessels. The
900 tumor cells migrate toward the blood vessels along the HGF gradient, adding directionality to the
901 migration of the tumor cell-macrophage paracrine loop engaged partners. **B)** In an inactive TMEM
902 doorway (box), with the absence of any CSF-1 secreted by the TMEM doorway tumor cell (TTC),
903 the VEGF-A remains within the TMEM doorway macrophage (TM). The blood vessels, including
904 the TMEM doorway endothelial cell (TEC) within the tumor remain sealed and do not allow tumor
905 cells to intravasate through TMEM doorways. **C)** In contrast, in an active TMEM doorway, CSF-1

906 is secreted by the TMEM doorway tumor cell and binds to macrophage CSF-1R, stimulating the
907 TMEM doorway macrophage to secrete its VEGF-A. VEGF-A causes vascular opening (TAVO
908 event) and allows tumor cells to intravasate through the TMEM doorway, creating CTCs, and
909 dextran or blood to leak out of the vessel. **D)** These circulating tumor cells (CTCs) travel through
910 the vasculature to secondary sites where TMEM doorways are also found in metastatic foci in
911 lymph nodes and lungs. Thin membranous connections between macrophages and tumor cells
912 stretch from the macrophage on extravascular side of the blood vessel through the endothelial
913 junctions and interact with CTCs which could facilitate CTC extravasation at secondary sites.
914 TMEM doorways in metastases could also be the sites were tumor cells re-intravasate and then
915 seed tertiary metastases. Figure created with BioRender.com.

Figure 1

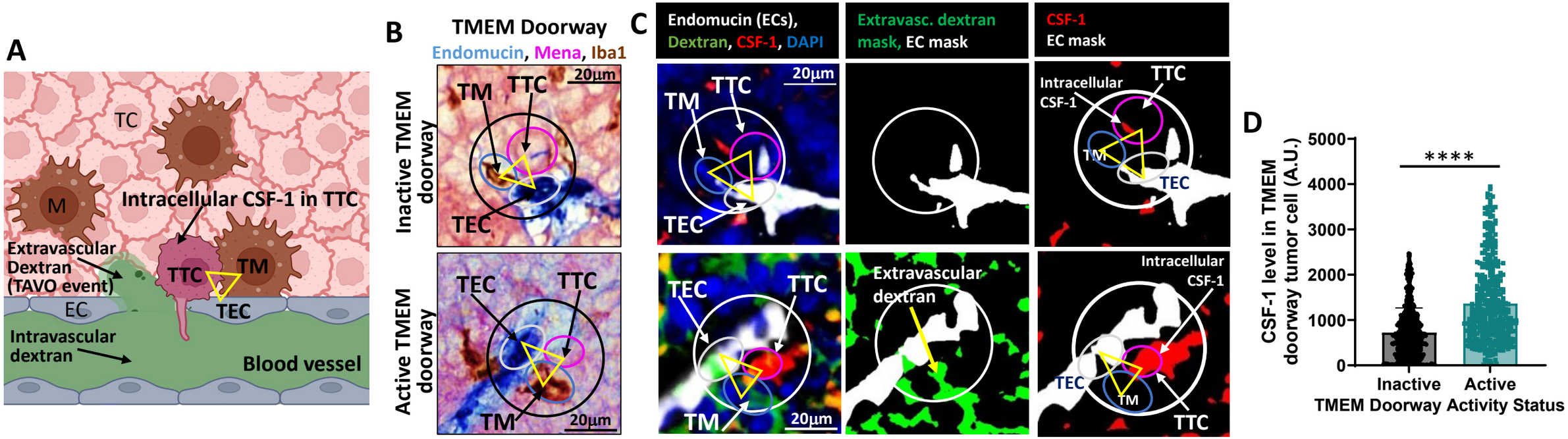
A
TC
M
Intracellular CSF-1 in TTC
Extravascular Dextran (TAVO event)
TTC
TM
EC
TEC
Intravascular dextran
Blood vessel
B
TMEM Doorway
Endomucin, Mena, Iba1
Inactive TMEM doorway
Active TMEM doorway
TM
TTC
TEC
20µm
C
Endomucin (ECs), Dextran, CSF-1, DAPI
Extravasc. dextran mask, EC mask
CSF-1 EC mask
Intracellular CSF-1
Extravascular dextran
D
CSF-1 level in TMEM doorway tumor cell (A.U.)
5000
4000
3000
2000
1000
0
****
Inactive
Active
TMEM Doorway Activity Status

Figure 2

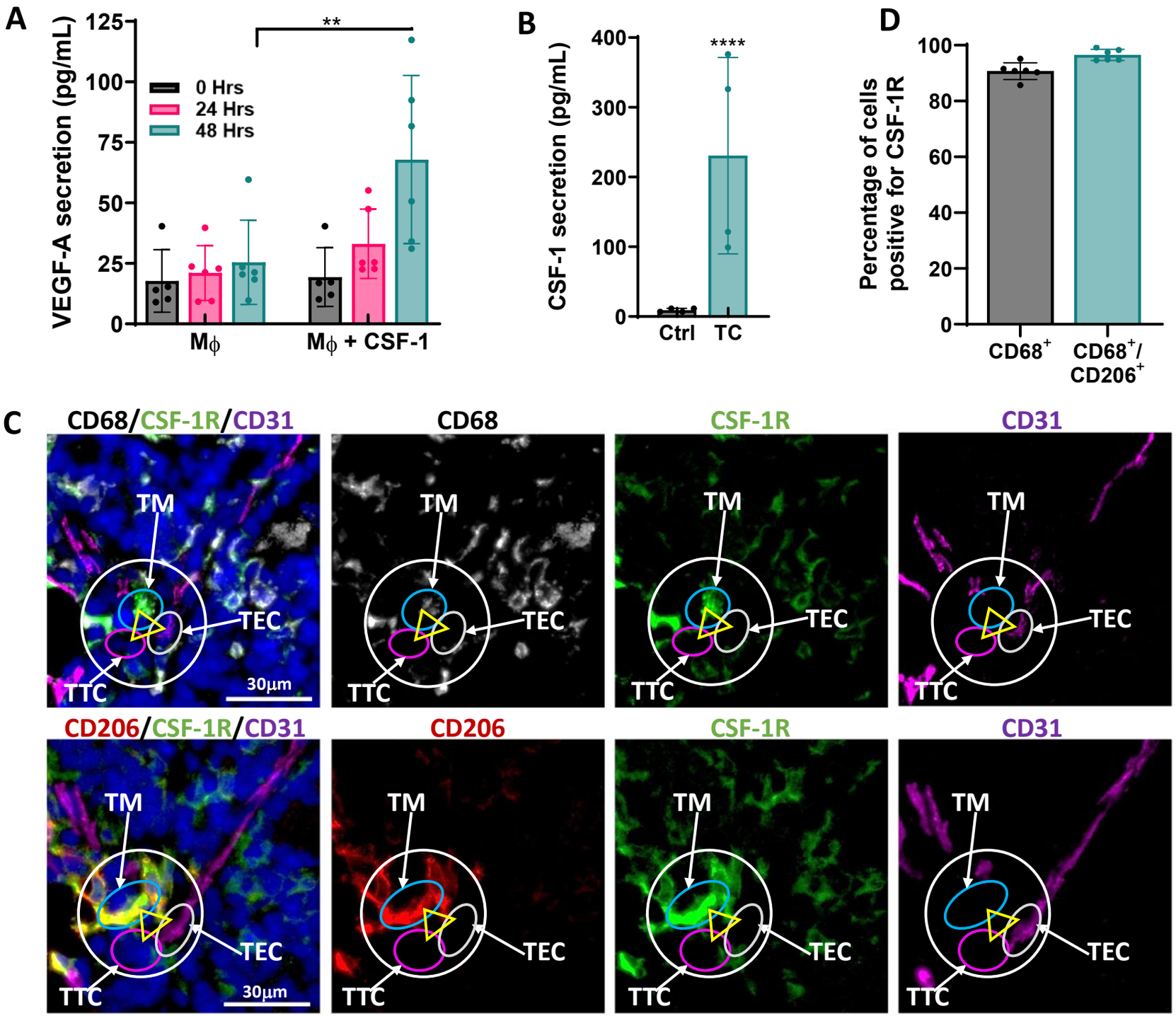
A
VEGF-A secretion (pg/mL)
125
100
75
50
25
0
**
0 Hrs
24 Hrs
48 Hrs
Mϕ
Mϕ + CSF-1
B
CSF-1 secretion (pg/mL)
400
300
200
100
0
****
Ctrl
TC
D
Percentage of cells positive for CSF-1R
100
80
60
40
20
0
CD68+
CD68+/ CD206+
C
CD68/CSF-1R/CD31
CD68
CSF-1R
CD31
CD206/CSF-1R/CD31
CD206
CSF-1R
CD31
TM
TEC
TTC
30µm

Figure 3

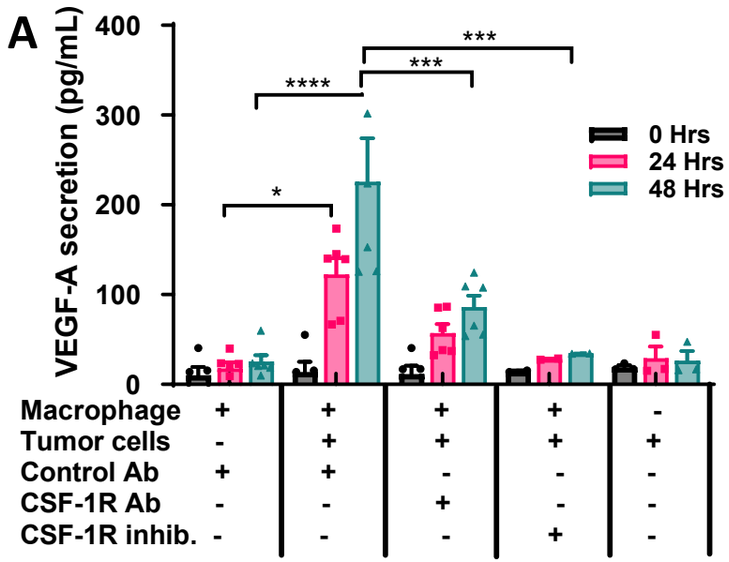
A
VEGF-A secretion (pg/mL)
400
300
200
100
0
*
****
***
***
0 Hrs
24 Hrs
48 Hrs
Macrophage + + + + -
Tumor cells - + + + +
Control Ab + + - - -
CSF-1R Ab - - + - -
CSF-1R inhib. - - - + -

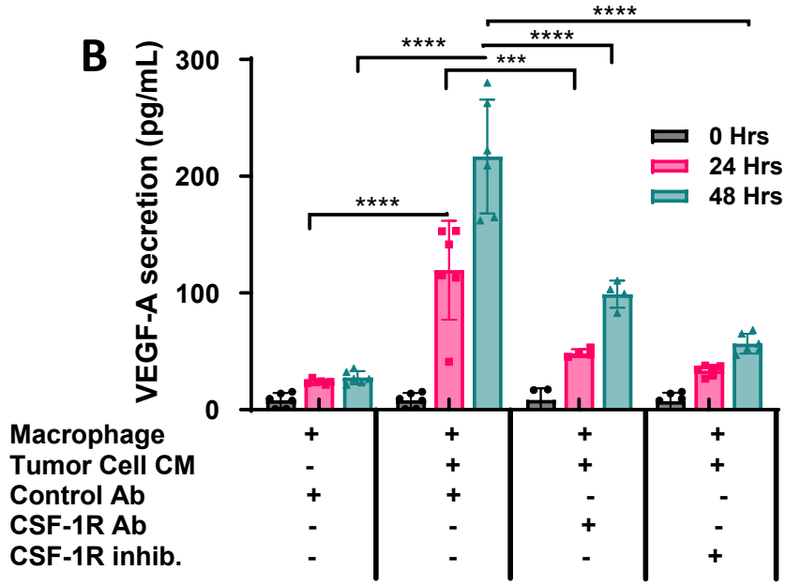
B
VEGF-A secretion (pg/mL)
300
200
100
0
****
****
****
***
****
0 Hrs
24 Hrs
48 Hrs
Macrophage + + + +
Tumor Cell CM - + + +
Control Ab + + - -
CSF-1R Ab - - + -
CSF-1R inhib. - - - +

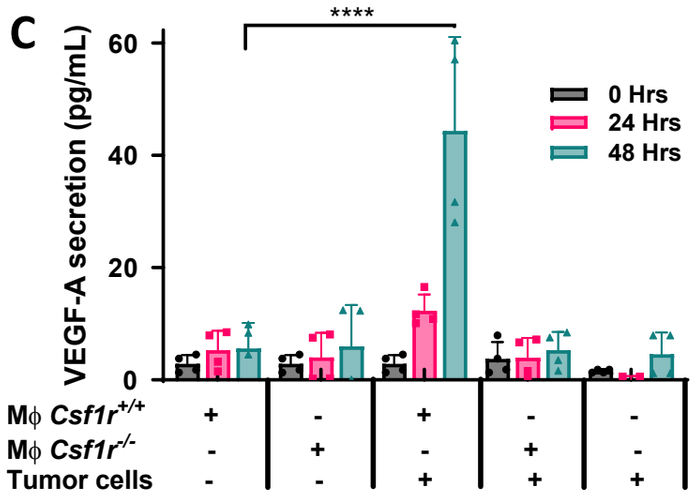
C
VEGF-A secretion (pg/mL)
60
40
20
0
****
0 Hrs
24 Hrs
48 Hrs
Mϕ Csf1r+/+ + - + - -
Mϕ Csf1r-/- - + - + -
Tumor cells - - + + +

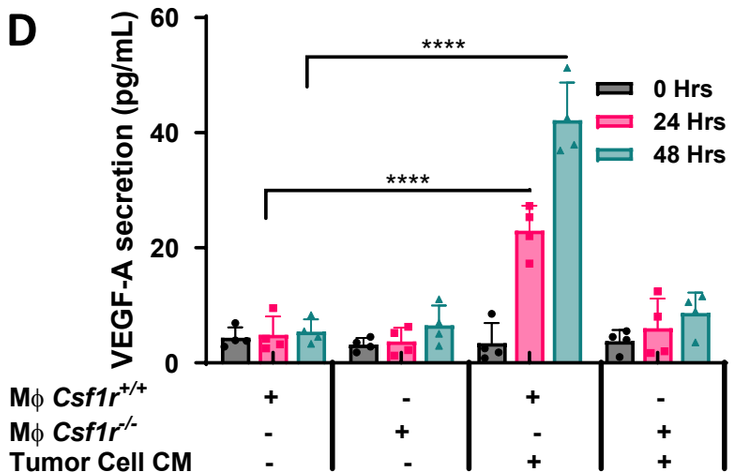
D
VEGF-A secretion (pg/mL)
60
40
20
0
****
****
0 Hrs
24 Hrs
48 Hrs
Mϕ Csf1r+/+ + - + -
Mϕ Csf1r-/- - + - +
Tumor Cell CM - - + +

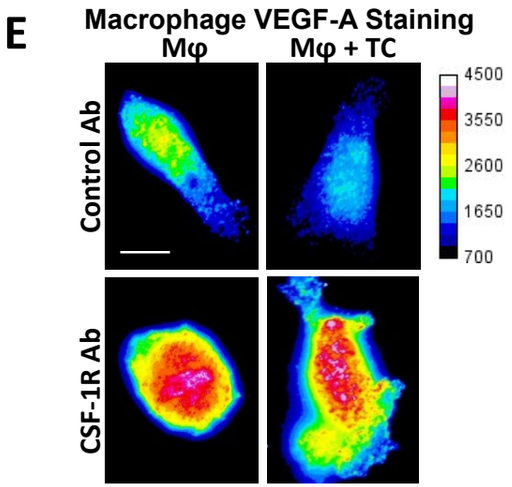
E
Macrophage VEGF-A Staining
Mφ
Mφ + TC
Control Ab
CSF-1R Ab
4500
3550
2600
1650
700

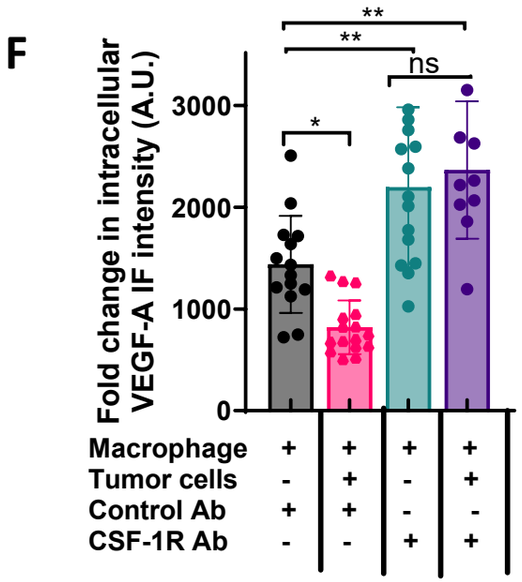
F
Fold change in intracellular VEGF-A IF intensity (A.U.)
3000
2000
1000
0
*
**
**
ns
Macrophage + + + +
Tumor cells - + - +
Control Ab + + - -
CSF-1R Ab - - + +

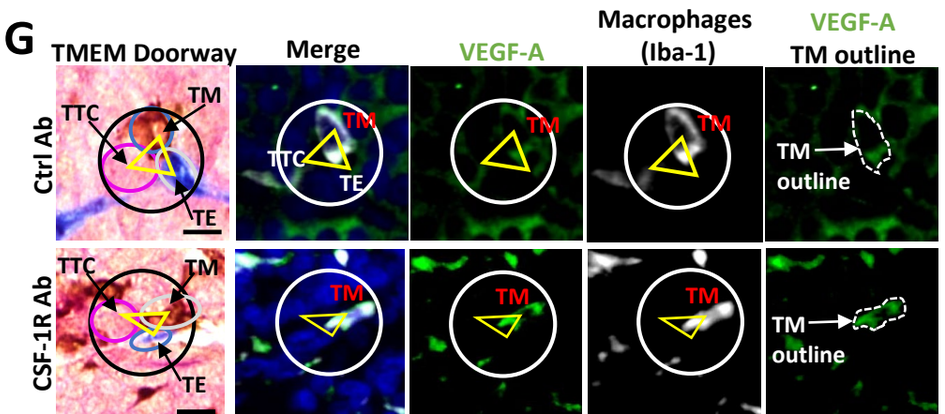
G
TMEM Doorway
Merge
VEGF-A
Macrophages (Iba-1)
VEGF-A
TM outline
Ctrl Ab
CSF-1R Ab
TTC
TM
TE
TM outline

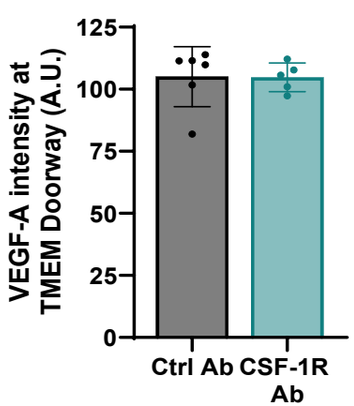
H
VEGF-A intensity at TMEM Doorway (A.U.)
125
100
75
50
25
0
Ctrl Ab
CSF-1R Ab

Figure 4

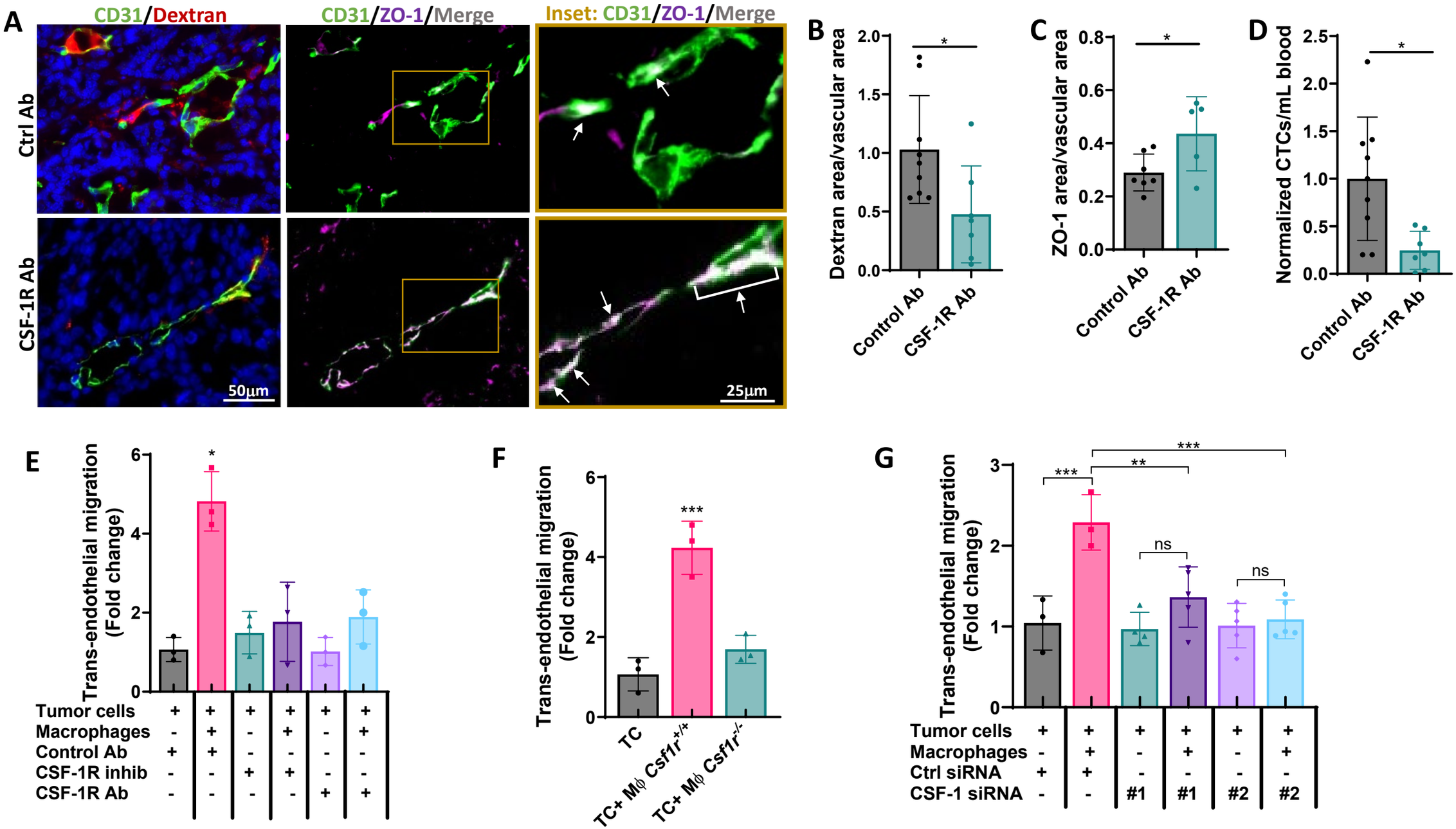
A
CD31/Dextran
CD31/ZO-1/Merge
Inset: CD31/ZO-1/Merge
Ctrl Ab
CSF-1R Ab
50µm
25µm
B
Dextran area/vascular area
Control Ab
CSF-1R Ab
C
ZO-1 area/vascular area
D
Normalized CTCs/mL blood
E
Trans-endothelial migration (Fold change)
Tumor cells
Macrophages
Control Ab
CSF-1R inhib
CSF-1R Ab
F
TC
TC+ Mϕ Csf1r+/+
TC+ Mϕ Csf1r-/-
G
Ctrl siRNA
CSF-1 siRNA
#1
#2
ns

Figure 5

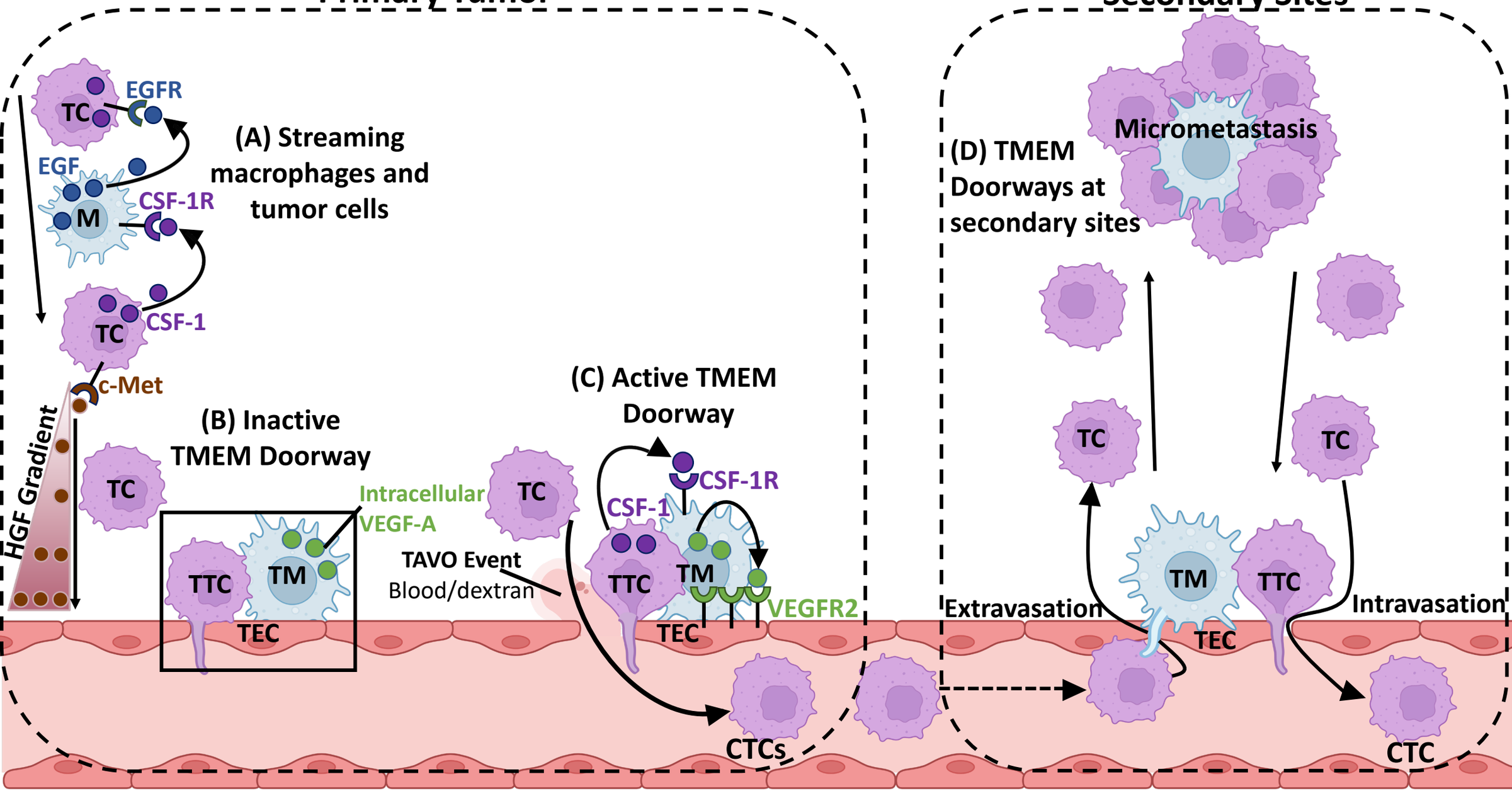
Primary Tumor
Secondary Sites
TC
EGFR
EGF
M
CSF-1R
(A) Streaming macrophages and tumor cells
TC
CSF-1
c-Met
HGF Gradient
(B) Inactive TMEM Doorway
TC
Intracellular VEGF-A
TTC
TM
TEC
TAVO Event
Blood/dextran
TC
(C) Active TMEM Doorway
CSF-1R
CSF-1
TTC
TM
VEGFR2
TEC
CTCs
(D) TMEM Doorways at secondary sites
Micrometastasis
TC
TC
TM
TTC
Extravasation
Intravasation
TEC
CTC